

**Meeting agricultural and environmental water demand in endorheic irrigated river basins
A simulation-optimization approach applied to the Urmia Lake basin in Iran**

Dehghanipour, Amir Hossein; Schoups, Gerrit; Zahabiyoun, Bagher; Babazadeh, Hossein

DOI

[10.1016/j.agwat.2020.106353](https://doi.org/10.1016/j.agwat.2020.106353)

Publication date

2020

Document Version

Accepted author manuscript

Published in

Agricultural Water Management

Citation (APA)

Dehghanipour, A. H., Schoups, G., Zahabiyoun, B., & Babazadeh, H. (2020). Meeting agricultural and environmental water demand in endorheic irrigated river basins: A simulation-optimization approach applied to the Urmia Lake basin in Iran. *Agricultural Water Management*, 241, Article 106353. <https://doi.org/10.1016/j.agwat.2020.106353>

Important note

To cite this publication, please use the final published version (if applicable).
Please check the document version above.

Copyright

Other than for strictly personal use, it is not permitted to download, forward or distribute the text or part of it, without the consent of the author(s) and/or copyright holder(s), unless the work is under an open content license such as Creative Commons.

Takedown policy

Please contact us and provide details if you believe this document breaches copyrights.
We will remove access to the work immediately and investigate your claim.

1 **Meeting agricultural and environmental water demand in endorheic irrigated river basins: a**
2 **simulation-optimization approach applied to the Urmia Lake basin in Iran**

3
4 Amir Hossein Dehghanipour^{a,*}, Gerrit Schoups^b, Bagher Zahabiyoun^{a,*}, Hossein Babazadeh^c

5 ^a *Department of Water Management, School of Civil Engineering, Iran University of Science and Technology, Tehran, Iran*

6 ^b *Department of Water Management, Faculty of Civil Engineering and Geosciences, Delft University of Technology, Delft, The Netherlands*

7 ^c *Department of Water Science and Engineering, Science and Research Branch, Islamic Azad University, Tehran, Iran*

8
9
10
11
12
13
14
15
16
17
18
19
20
21
22
23
24
25
26
27
28
29
30
31
32
33
34
35
36
37
38
39
40
41
42
43
44

* Corresponding author address: Department of Water Management, School of Civil Engineering, Iran University of Science and Technology, Narmak, Tehran, Iran, Postal Code: 16846-13114.

E-mail: A.Dehghanipour@tudelft.nl (A.H. Dehghanipour), Bagher@iust.ac.ir (B. Zahabiyoun)

¹Present address: Department of Water Management, Faculty of Civil Engineering and Geosciences, Delft University of Technology, Stevinweg 1, 2628CN, Delft, Netherlands. Tel:+31618838382

45
46
47
48
49
50
51
52

Highlights

- Simulation-optimization approach for water management in irrigated endorheic basins
- Spatially distributed simulation of surface water and groundwater resources
- Multi-objective optimization to meet environmental and agricultural water demand
- Conjunctive use and time-variable environmental flow requirements to tackle droughts
- Sustainable water management strategies for the Lake Urmia basin

Abstract

43 Competition for water between agriculture and the environment is a growing problem in irrigated regions across the
44 globe, especially in endorheic basins with downstream freshwater lakes impacted by upstream irrigation
45 withdrawals. This study presents and applies a novel simulation-optimization (SO) approach for identifying water
46 management strategies in such settings. Our approach combines three key features for increased exploration of
47 strategies. First, minimum environmental flow requirements are treated as a decision variable in the optimization
48 model, yielding more flexibility than existing approaches that either treat it as a precomputed constraint or as an
49 objective to be maximized. Second, conjunctive use is included as a management option by using dynamically
50 coupled surface water (WEAP) and groundwater (MODFLOW) simulation models. Third, multi-objective
51 optimization is used to yield entire Pareto sets of water management strategies that trade off between meeting
52 environmental and agricultural water demand. The methodology is applied to the irrigated Miyandoab Plain,
53 located upstream of endorheic Lake Urmia in Northwestern Iran. Results identify multiple strategies, i.e.,
54 combinations of minimum environmental flow requirements, deficit irrigation, and crop selection, that
55 simultaneously increase environmental flow (up to 16%) and agricultural profit (up to 24%) compared to historical
56 conditions. Results further show that significant temporary drops in agricultural profit occur during droughts when
57 long-term profit is maximized, but that this can be avoided by increasing groundwater pumping capacity and
58 temporarily reducing the lake's minimum environmental flow requirements. Such a strategy is feasible during
59 moderate droughts when resulting declines in groundwater and lake water levels fully recover after each drought.
60 Overall, these results demonstrate the usefulness and flexibility of the methodology in identifying a range of
61 potential water management strategies in complex irrigated endorheic basins like the Lake Urmia basin.

62 **Keywords:** *Environmental flow requirement; Conjunctive use; WEAP; MODFLOW; Multi-Objective Optimization; Drought.*

1. Introduction

63 Irrigated agriculture is the largest consumer of water resources, accounting for approximately 70% of all
64 freshwater extraction from surface water (SW) and groundwater (GW) resources (Malano and Davidson,
65 2009; Molden, 2013; Pang et al., 2014, 2013; Singh, 2014). Large agricultural water demand competes
66 with other water demands, in particular environmental flow requirements to sustain natural ecosystems
67 (Jägermeyr et al., 2017; Malano and Davidson, 2009; Pang et al., 2014; Xue et al., 2017). Environmental
68 flow requirement is defined as river flow that is necessary to sustainably maintain ecological health of
69 natural ecosystems, such as wetlands and lakes (Arthington et al., 2018; Smakhtin et al., 2006; Yasi and
70 Ashori, 2017). In many parts of the world, increased water consumption for irrigation has led to mounting
71 pressure on available water resources to meet environmental flow requirements and has resulted in

85 growing conflicts between agricultural and environmental water demand (Dunn et al., 2003; Xue et al.,
86 2017). These conflicts are exacerbated by climate change, drought, and water mismanagement, especially
87 in arid and semi-arid regions (Mancosu et al., 2015; Valipour, 2015; Valipour et al., 2015). Many of the
88 adverse effects of decreasing environmental water flow have led to the degradation of natural aquatic
89 bodies, such as lakes, wetlands, and oases (Sisto, 2009).

90 Endorheic river basins, usually located in arid and semi-arid regions, are particularly sensitive to
91 competition between agricultural and environmental water demand (Wang et al., 2018). Rivers in
92 endorheic basins do not discharge into the ocean but rather in terminal lakes whose water supplies are
93 sensitive to upstream water extractions and to natural climatic variations such as droughts (Wang et al.,
94 2018). Therefore, maintaining and sustaining environmental flow requirements is a high priority in these
95 basins (Yapiyev et al., 2017) and conflict between agricultural demand and environmental flow
96 requirements in endorheic basins, especially during droughts, has been a focus of various studies (Bai et
97 al., 2012; Chunyu et al., 2019). During the 20th and 21st centuries, SW extraction for irrigated agriculture
98 significantly increased in endorheic river basins, especially in arid and semi-arid regions. Furthermore,
99 the adverse impact of climate change and drought in these regions reduced downstream outflow from
100 rivers, resulting in shrinking and drying up of terminal lakes (Cai and Rosegrant, 2004; Chunyu et al.,
101 2019; Farrokhzadeh et al., 2020; Rumbaur et al., 2015). For instance, the surface area of Lake Chad that
102 is located in the most extensive African endorheic basin, shrank by 90% over the last 40 years (Lemoalle
103 et al., 2012; Yapiyev et al., 2017), while the surface area of Lake Aral in Central Asia decreased by 75%
104 from 1975 to 2007 (Bai et al., 2011; Pritchard, 2017; Yapiyev et al., 2017).

105 Tharme (2003) reviewed existing methods for calculating environmental flow requirements worldwide.
106 The results of this study indicate that 207 different methodologies exist for calculating environmental
107 flow requirements. A disadvantage of these methods is that other water demands that may exist in the
108 basin, e.g. agricultural water demand, are not taken into account which means that the calculated
109 environmental flow requirements are difficult to achieve in practice and be accepted by stakeholders
110 (Barbier et al., 2009; Mainuddin et al., 2007; O’Keefe, 2009; Pang et al., 2014; Wei et al., 2009).

111 A more holistic approach considers environmental flow requirements and agricultural water demand
112 together. This path has been explored by various studies. For instance, Munoz-Hernandez et al. (2011)
113 developed a simulation model to investigate the impact of three alternative environmental water
114 allocation strategies on agricultural profits in the Rio Yaqui basin, Mexico. Other studies used a
115 simulation-optimization (SO) model to find water allocation strategies that simultaneously meet
116 environmental flow requirements and water demand from agriculture and other users (see Table S1). A
117 first distinction among these studies relates to the way minimum environmental flow requirements are
118 estimated: either fixed based on historical streamflow records (e.g., Xevi and Khan, 2005), treated as a
119 function of reservoir water storage (e.g. (Anghileri et al., 2013)), or set to a fixed fraction of river

120 discharge (e.g., Fallah-Mehdipour et al., 2020, 2018; Hu et al., 2016). The latter approach is known as the
121 Tennant method (Tennant, 1976). A second distinction among existing SO studies relates to how
122 environmental flow requirements are included in the optimization model: either as a firm constraint (e.g.,
123 Anghileri et al., 2013; Hu et al., 2016; Pulido-Velazquez et al., 2008; Xevi and Khan, 2005), or as an
124 objective function to be maximized (e.g., Fallah-Mehdipour et al., 2020, 2018; Yang and Yang, 2014).
125 Building on these previous studies, this paper investigates application of SO modeling for resolving
126 competition between environmental flows and agricultural demand in the 1524 km² Miyandoab Plain, an
127 irrigated plain in the Urmia Lake Basin, a cold-semi-arid endorheic basin in the northwest of Iran. There
128 are several complex water problems in the Miyandoab Plain due to drought and water mismanagement.
129 Overuse of irrigation in the basin coupled with a recent drought has resulted in decreased environmental
130 flows to Lake Urmia and led to continued shrinking of the lake (Hosseini-Moghari et al., 2018; Moshir
131 Panahi et al., 2020; Schulz et al., 2020). As such, environmental flow requirements for Urmia lake are in
132 direct competition with agricultural water demand. In this regard, the Iranian government has established
133 the Urmia Lake Restoration Program (ULRP) to explore strategies of water consumption reduction and
134 increased efficiency and productivity in the agricultural sector (Shadkam et al., 2016). However,
135 strategies should be designed so that farmers do not suffer income losses. A previous study by
136 Ahmadzadeh et al. (2016) has shown that improvements in irrigation efficiency have little effect in an
137 endorheic basin like the Lake Urmia basin, suggesting the need for other strategies such as changes in
138 crop acreage and crop patterns, and the application of deficit irrigation for decreasing agricultural water
139 consumption and increasing total inflow to the lake (Ahmadzadeh et al., 2016). An additional strategy for
140 resolving temporary water shortage during droughts that has not yet been explored in the Miyandoab
141 Plain consists of conjunctive use of SW and GW resources (Tian et al., 2015), a strategy that has been
142 applied successfully in other regions (e.g., Peralta et al., 1995; Karamouz et al., 2004; Xevi and Khan,
143 2005; Schoups et al., 2005; Schoups et al., 2006; Safavi et al., 2010; Singh and Panda, 2013; Seo et al.,
144 2018).

145 The goal of our study is to present a novel SO approach for reconciling competing agricultural and
146 environmental water demands, and apply this methodology for finding potential water management
147 strategies that meet environmental flow requirements to Urmia lake while improving and enhancing the
148 agricultural economy in the upstream Miyandoab Plain. Our study contributes both novel methodology
149 and novel insights into water management in the application case study. In terms of methodology, our
150 paper extends existing studies in at least three different ways. First, while previous SO approaches
151 included environmental flow either as constraint or as objective function in the optimization, here we
152 introduce and test an alternative approach that treats minimum environmental flow requirements as a
153 separate decision variable in the optimization. This approach introduces additional flexibility for finding
154 better water management strategies. Second, our SO model includes both SW and GW components, and

155 as such provides a larger solution space for exploring sustainable water management strategies, e.g.
156 strategies where agriculture increases GW use to reduce SW extractions and meet environmental SW
157 flow requirements. The hydrologic module in our SO model is based on a recently developed WEAP-
158 MODFLOW model of the Miyandoab Plain (Dehghanipour et al., 2019) that includes coupled water
159 balances for all relevant system components, i.e. the root zone, surface water reservoir, river, canals, and
160 the underlying aquifer. Third, multi-objective optimization is used to yield entire Pareto sets of water
161 management strategies that trade-off between meeting environmental and agricultural water demand. In
162 terms of application, our study builds on the recommendations of (Ahmadzadeh et al., 2016) by
163 investigating new strategies for solving the water management problems in Miyandoab Plain that include
164 changes in crop acreage, changes in crop pattern, and application of deficit irrigation.

165 The paper is divided into five sections. Section 2 introduces the study area, i.e. the Miyandoab Plain in
166 the Urmia Lake basin. Section 3 presents the simulation-optimization model, including a discussion of the
167 hydrologic, agronomic, and economic modules of the simulation model, as well as a description of the
168 decision variables, constraints, and objective functions of the optimization model. Section 4 provides
169 results of the simulation-optimization model for identifying sustainable water allocation strategies that
170 meet agricultural water demand and environmental flow requirements in the Miyandoab Plain. Section 5
171 summarizes conclusions of the study.

172 **2. Case study**

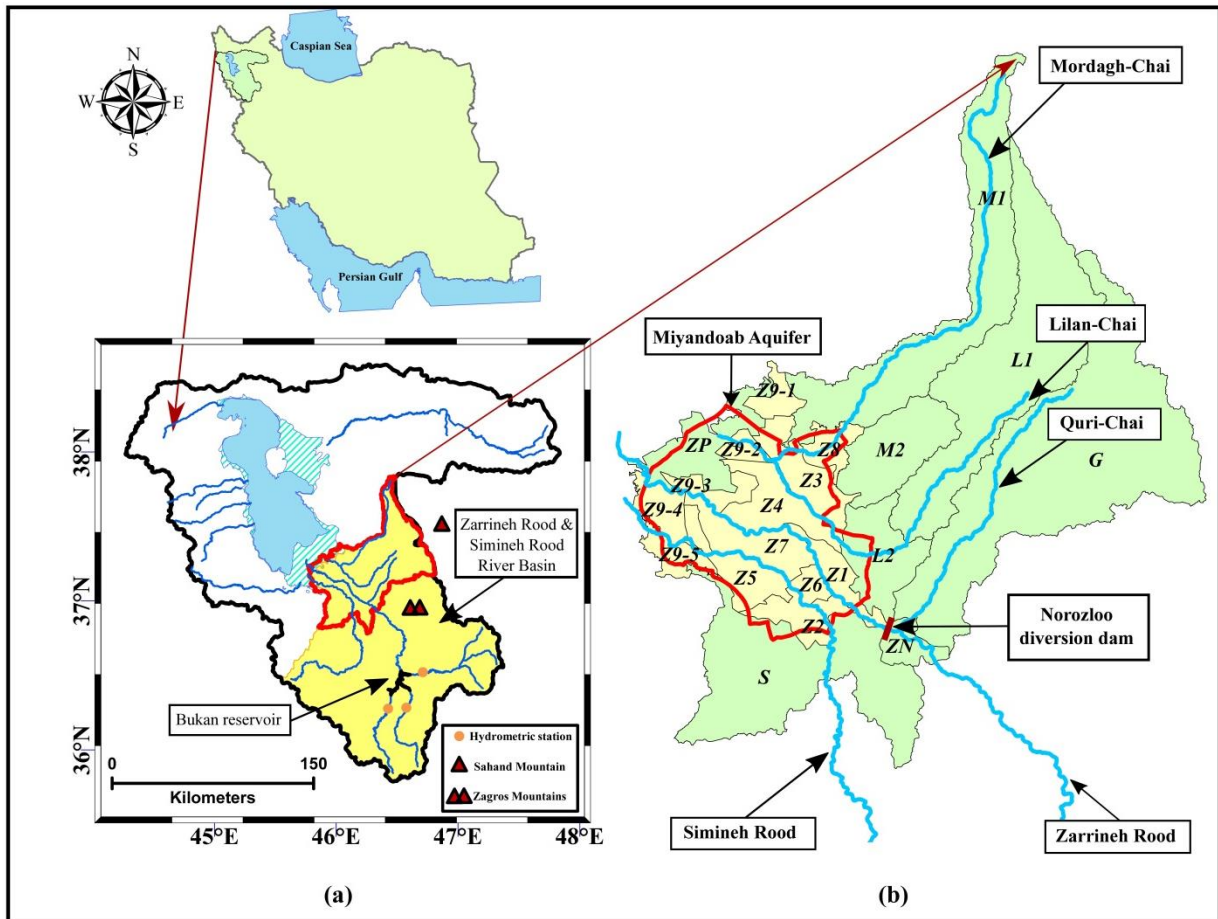
173 **2.1. GW and SW resources, hydrology and hydrogeology**

174 The Miyandoab Plain is an agricultural region located in the northwest of Iran in the Urmia basin (Fig.
175 1.a), between the Zagros mountains, the Sahand mountains, and Lake Urmia. The region has a semi-arid-
176 cold climate and average annual precipitation of ~290mm, most of which falls from October to May.
177 Annual temperature and reference evapotranspiration average 14°C and 1170 mm, respectively. The
178 population of the Miyandoab Plain equals 255,841 and consists of 70,251 households, with 64%
179 employment in the agricultural sector (Ministry of Energy of Iran, 2016).

180 The Miyandoab Plain is divided into 21 agricultural zones (Fig. 1.b) which are characterized as either
181 “internal” (with irrigation and drainage canals) or “external” (without irrigation and drainage canals). The
182 total area of all agricultural zones is approximately 100,000 hectares, consisting of orchards (42%) and
183 crops (52%). Orchards consist of apple, grapes, stone-fruits, almond, and conifer trees, which are
184 cultivated from March to October. Crops include wheat, maize, alfalfa, sugar beet, and tomato, each with
185 their own distinctive growing season (Fig. S1). Crops and orchards are irrigated using a combination of
186 SW and GW resources.

187 The SW system consists of main rivers and their tributaries, reservoirs, and irrigation and drainage canals.
188 The main rivers are Zarrineh Rood, Simineh Rood, Mordaq-Chai, Lilan-Chai, and Quri-Chai, with
189 average annual runoff of 1460, 326, 75, 64, and 41 MCM, respectively (Fig. 1.b). Zarrineh Rood and

190 Simineh Rood are the most important rivers in Urmia Basin: they provide more than 50% of total annual
 191 environmental flows into Urmia Lake (Ghaheri et al., 1999). The biggest reservoir in the Urmia basin,
 192 Bukan reservoir, is located on the Zarrineh Rood river (Fig. 1.a) and has a total storage volume that was
 193 increased in the year 2008 from 650 to 808 MCM, with 130 MCM of dead storage. SW releases from
 194 Bukan reservoir are conveyed to the internal zones via the Norozloo diversion dam and a network of
 195 primary irrigation canals (Fig. 1.b).



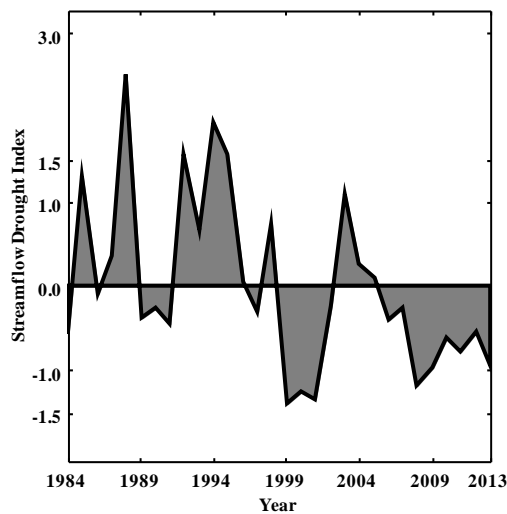
196
 197 **Fig. 1: Location of the study area (a) Miyandoab Plain in the Urmia basin, Iran (b) Agricultural zones in Miyandoab**
 198 **Plain and Miyandoab aquifer. Internal and external zones are shown in yellow and green, respectively.**
 199

200 The internal agricultural zones are underlain by the Miyandoab aquifer (Fig. 1.b). The aquifer is
 201 unconfined, and has a small specific yield (on average about 0.035). Twenty-two thousand (22,000) wells
 202 with a total annual capacity of approximately 140 MCM are operational in Miyandoab aquifer to supply
 203 additional water for irrigation.

204 Land slope of the internal zones is very low, and irrigation and drainage canals and pumping wells have
 205 been extensively developed in the internal zones. These facilities have led to cultivation of most of the
 206 land in the internal zones. External zones, on the other hand, consist of mountains and foothills without
 207 extensive aquifers. Therefore, agricultural land in the external zones is concentrated along rivers and is
 208 irrigated using SW from river diversions and GW from local shallow groundwater along rivers.

209 **2.2. Historical hydrologic droughts in Miyandoab Plain**

210 Fig. S2 shows a time series of annual river discharge upstream of Bukan reservoir (Fig. 1.a), and Fig. 2
 211 shows the corresponding Streamflow Drought Index (SDI), calculated according to Nalbantis and Tsakiris
 212 (2009). These data show multi-year droughts (negative SDI) from 1999 to 2002 and from 2006 to 2013.
 213 In comparison, the period before 1998 was markedly wetter. Table 1 further indicates that 1999, 2000,
 214 2001, and 2008 were the driest years in the region. Upstream river discharge for these years was 31% of
 215 the average upstream river discharge during 1984-2013. These reductions in upstream inflow directly
 216 increase competition between sustaining downstream environmental flow to Lake Urmia and sustaining
 217 the agricultural economy in Miyandoab Plain. Our goal is to explore water management strategies that
 218 alleviate this competition, especially during droughts when water supplies are limited.



219

220 **Fig. 2: Annual time series of Streamflow Drought Index (SDI) for upstream inflow into Bukan reservoir**

221

222

223

Table 1: Classification of hydrologic drought years in Miyandoab Plain based on the SDI (Nalbantis and Tsakiris, 2009) in Fig. 2

Classification	Identifier	Criterion	Years of occurrence
Non-drought	HD1	$0.0 \leq \text{SDI}$	1985, 1987, 1988, 1992, 1993, 1994, 1995, 1996, 1998, 2003, 2004, 2005
Mild drought	HD2	$-1.0 \leq \text{SDI} < 0.0$	1984, 1986, 1989, 1990, 1991, 1997, 2002, 2006, 2007, 2009, 2010, 2011, 2012, 2013
Moderate drought	HD3	$-1.5 \leq \text{SDI} < -1$	1999, 2000, 2001, 2008
Severe drought	HD4	$-2.0 \leq \text{SDI} < -1.5$	---
Extreme drought	HD5	$\text{SDI} < -2.0$	---

224

225 2.3. Current and proposed crop pattern in the Miyandoab Plain

226 As mentioned in the introduction, the ULRP has developed scenarios for the reduction of water
 227 consumption in the agricultural sector. The ULRP has proposed a new crop pattern for the Miyandoab
 228 Plain (Fig. 3), aimed at reducing agricultural water consumption and increasing agricultural profits
 229 (Ministry of Energy of Iran, 2016). The proposed crop pattern is the output of a Multi-Objective Decision
 230 Making (MODM) model in which economic and environmental goals are considered. This model seeks to
 231 increase agricultural income, reduce cultivation costs, maintain market share, and increase environmental
 232 flow to Lake Urmia. The constraints considered in this modeling include the following:

- Reducing the area of orchards is costly. Moreover, reducing the area of orchards leads to an increase in unemployment with important social consequences. Therefore, in the proposed crop pattern, the area and pattern of orchards remain unchanged.
- The maximum irrigation demand of the proposed crop pattern is equal to the irrigation demand in the current crop pattern.
- The minimum agricultural profit for the proposed crop pattern is equal to agricultural profit for the current crop pattern.
- Wheat is a staple crop to guarantee food security and is widely cultivated in the Miyandoab Plain. Moreover, wheat has a relatively low water demand (Table S2). The area occupied by wheat was therefore not changed and remains at 55%.
- Sugar beet, tomato, and alfalfa have relatively high water demands (Table S2). In the proposed crop pattern, the areas of these crops were decreased to an extent that does not jeopardize economic activities that depend on these crops, i.e. sugar processing factories, tomato paste factories, and livestock.
- Finally, the proposed crop pattern introduces new low water demand crops such as rapeseed, saffron, and sorghum (Table S2). Saffron and sorghum are high-value crops with a large water productivity (Table S3).

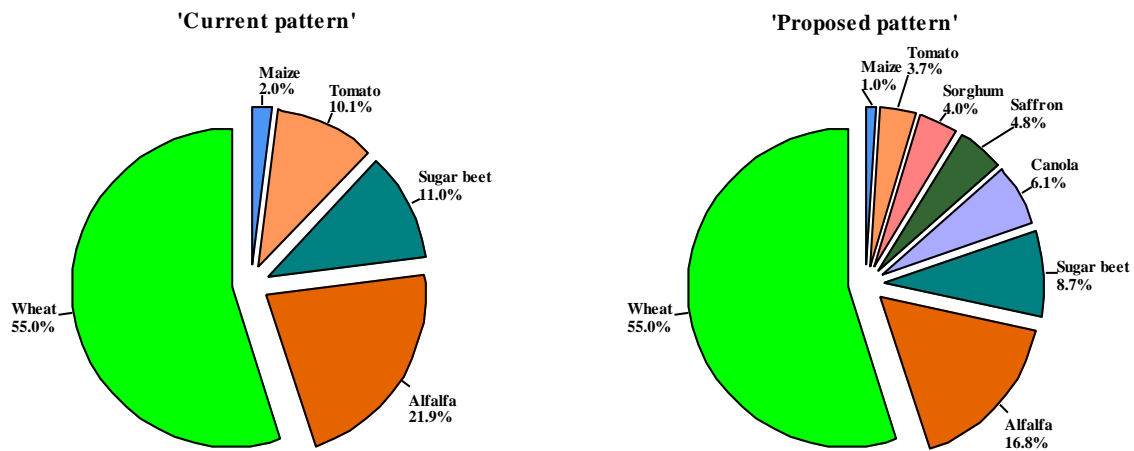
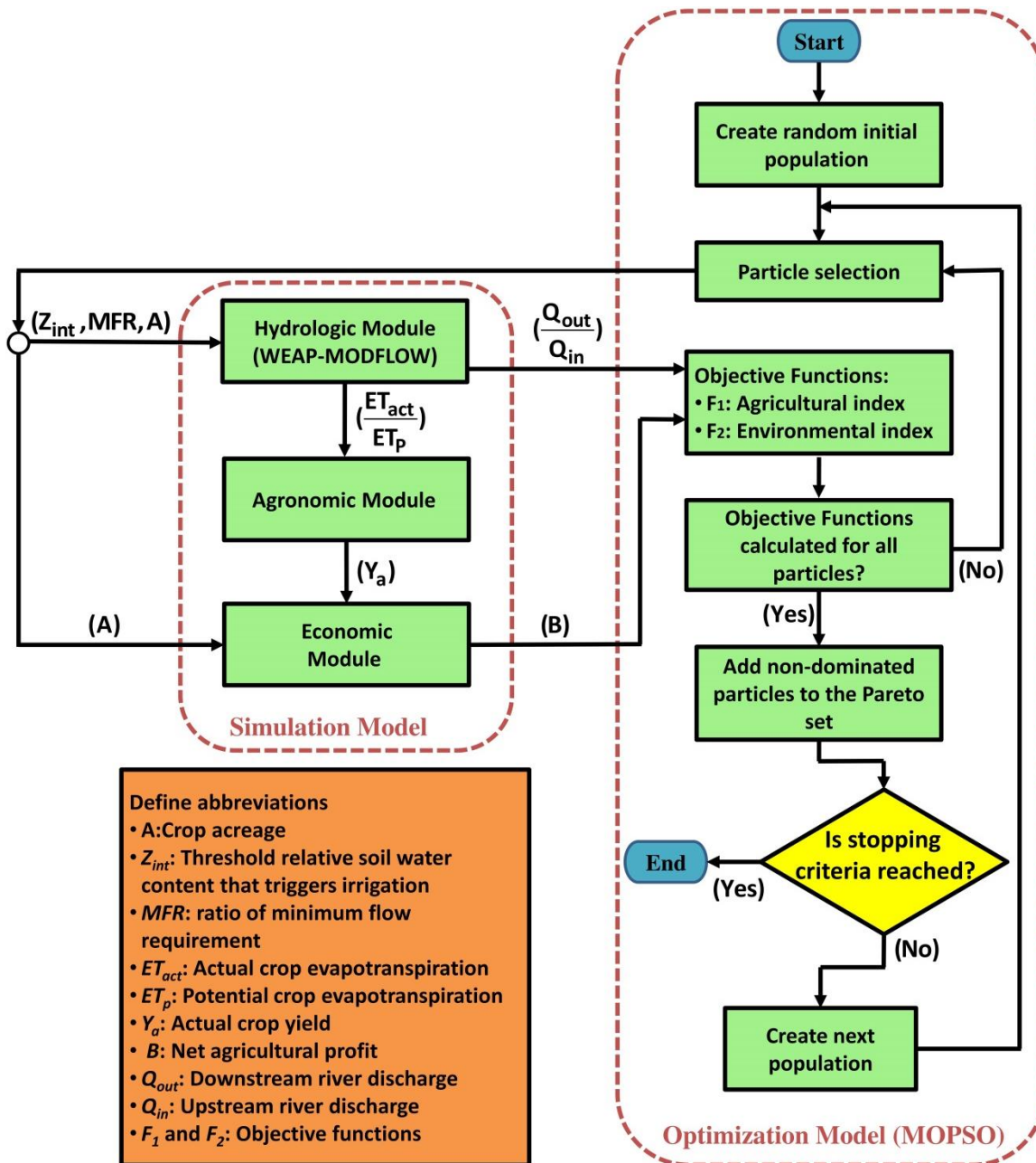


Fig. 3: Current and proposed crop patterns in the Miyandoab Plain (Ministry of Energy of Iran, 2016)

3. Integrated SW-GW Simulation-Optimization Model

In this study, an integrated SW-GW SO model was developed to evaluate different management scenarios in the Miyandoab Plain that achieve sustainable agricultural production without compromising

261 environmental flows to Lake Urmia. An outline of the SO model is shown in Fig. 4. This figure shows
262 how the simulation model interacts with the optimization model. The simulation component consists of
263 three modules: (1) a *hydrologic module* for computing SW-GW flows and storages, (2) an *agronomic*
264 *module* for computing crop yields, and (3) an *economic module* for computing agricultural profits. The
265 optimization model consists of two conflicting objective functions: *Agricultural index* and *Environmental*
266 *index*. We used multi-objective optimization based on the Multi-Objective Particle Swarm Optimization
267 (MOPSO) algorithm (Coello et al., 2004) to yield entire Pareto sets of water management strategies that
268 trade off between conflicting objective functions. The SO modeling steps are as follows: The optimization
269 model creates a new population of particles, where each particle represents a set of decision variables for
270 the period 1984-2013. The period 1984-2013 is divided into three hydrological droughts period based on
271 Table 1, and decision variables consist of *crop acreage* (A), the *threshold relative soil water content that*
272 *triggers irrigation* (Z_{int}), and the *ratio of minimum flow requirement* (MFR) for each hydrological drought
273 conditions. Each particle (i.e., set of decision variables for three hydrological droughts periods) provides
274 input to the simulation model. After that, the hydrologic module in the simulation model runs once and
275 for the entire simulation period (1984-2013) on a monthly time scale. Monthly *actual crop*
276 *evapotranspiration* (ET_{act}) and *potential crop evapotranspiration* (ET_p) are outputs of the hydrologic
277 module, and they are imported to the agronomic module. Moreover, monthly *downstream river discharge*
278 (inflow into Urmia lake, Q_{out}) and monthly *upstream river discharge* (Q_{in}) are other outputs of the
279 hydrologic module, and they are sent to the optimization model for calculating the environmental index.
280 The agronomic module simulates *actual crop yield* (Y_a) for each crop in each water year and this result is
281 sent to the Economic module to calculate net *agricultural profit* (B). The net agricultural profit is sent to
282 the optimization model to calculate the agricultural index. The process is repeated for each particle in the
283 current population. Finally, non-dominated particles in the population are saved and added to the Pareto
284 set. If the stopping criterion of the optimization model is not reached, a new population of particles is
285 generated by the optimization algorithm, and the entire procedure is repeated. Therefore, the optimization
286 component runs the simulation modules to determine values for the *decision variables* that maximize the
287 *objective functions*, subject to a set of physical *constraints*. In the following sections, we discuss the
288 various parts of the SO model in more detail.



289

290

291

Fig. 4: Outline of the integrated SW-GW Simulation-Optimization model. Each particle in the optimization algorithm represents a set of decision variables.

292

293

294

295

296

297

298

299

300

301

302

303

304

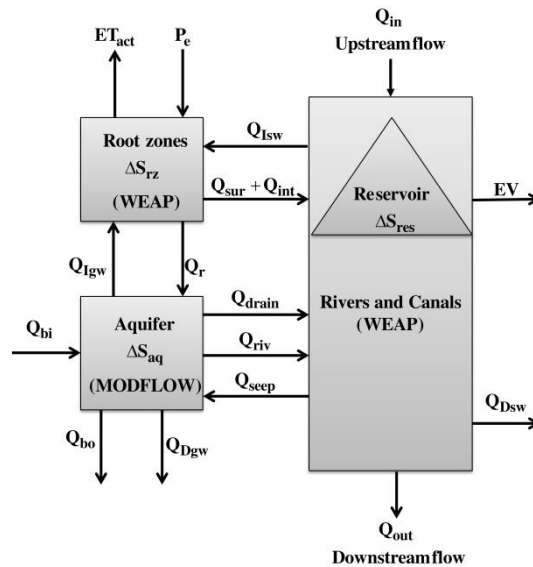
305

306 **3.1. Hydrologic Module**

307 The hydrologic module is based on the integrated SW-GW model described in Dehghanipour et al.
 308 (2019), who developed a WEAP-MODFLOW model for the Miyandoab Plain. The hydrologic module
 309 consists of three interacting spatially distributed water balance components: 1) the crop root zone, 2) the
 310 SW system (rivers, surface reservoirs, and irrigation and drainage canals), and 3) the underlying aquifer
 311 (Dehghanipour et al., 2019). Fig. 5 shows a schematic diagram of interacting control volumes for all
 312 components of the hydrologic module. The monthly water balance is applied to each of the components
 313 as follows:

314
$$\frac{\Delta S}{\Delta t} = \sum Q_i - \sum Q_o \quad (1)$$

315 where ΔS is change in water storage (L^3), $\sum Q_i$ is total input (L^3/T) and $\sum Q_o$ is total output (L^3/T).
 316 Table 2 summarizes the water balance equation for each physical component and its variables. The
 317 hydrologic module was implemented using a dynamic coupling between WEAP and MODFLOW
 318 (Harbaugh, 2005; Purkey et al., 2009; Sieber and Purkey, 2015). More details about variables, equations,
 319 and implementation of the hydrologic module are presented in Dehghanipour et al. (2019), who showed
 320 that the model successfully mimics historically observed river discharge and groundwater levels.



321
 322 **Fig. 5: Schematic diagram of the coupled SW-GW flow model. Variables are defined in Table 2. Each model component**
 323 **is spatially discretized into interacting control volumes for which monthly water balances are formulated**
 324 **(Dehghanipour et al., 2019).**
 325
 326
 327
 328
 329
 330
 331
 332
 333
 334
 335

Table 2: Monthly water balance variables and equations for spatially distributed model components shown in Fig. 5.

Variable	Unit	Equation or data source
Storage change in the root zone of each agricultural zone	L ³ /T	$\frac{\Delta S_{rz}}{\Delta t} = nZ_r A_{rz} \frac{\Delta z}{\Delta t} = Q_{Isw} + Q_{Igw} + P_e A_{rz} - ET_{act} A_{rz} - Q_{sur} - Q_{int} - Q_r$
Storage change in each aquifer grid cell	L ³ /T	$\frac{\Delta S_{aq}}{\Delta t} = A_{aq} S_y \Delta h = Q_r + Q_{seep} + Q_{bi} - Q_{Igw} - Q_{Dgw} - Q_{riv} - Q_{drain} - Q_{bo}$
Storage change in Bukan reservoir	L ³ /T	$\frac{\Delta S_{res}}{\Delta t} = Q_{in} - R + A_{res} P_{res} - A_{res} EV$
Downstream river discharge	L ³ /T	$Q_{out} = Q_{in} - Q_{Isw} - Q_{Dsw} - Q_{seep} + Q_{riv} + Q_{sur} + Q_{int} + Q_{drain}$
SW extraction for irrigation	L ³ /T	Q_{Isw}
GW extraction for irrigation	L ³ /T	Q_{Igw}
Effective precipitation	L/T	P_e
Irrigated area for each crop in each zone	L ²	A_{rz}
Actual evapotranspiration	L/T	ET_{act}
Surface runoff	L ³ /T	Q_{sur}
Inte rflow	L ³ /T	Q_{int}
GW recharge	L ³ /T	Q_r
Seepage from river	L ³ /T	Q_{seep}
Lateral GW flows	L ³ /T	Q_{bi}, Q_{bo}
GW extraction for drinking	L ³ /T	Q_{Dgw}
GW discharge to river	L ³ /T	Q_{riv}
GW discharge to drain	L ³ /T	Q_{drain}
Grid cell area of aquifer	L ²	$A_{aq} = (500 \text{ m})^2$
Upstream river discharge	L ³ /T	Q_{in}
Downstream river discharge	L ³ /T	Q_{out}
Downstream release from Bukan reservoir	L ³ /T	R
Precipitation rate on Bukan reservoir	L/T	P_{res}
Bukan reservoir surface area	L ²	A_{res}
Evaporation rate from Bukan reservoir	L/T	EV
SW extraction for drinking water	L ³ /T	Q_{Dsw}
Relative soil water content	-	z
Rooting depth	L	Z_r
hydraulic head (GW level)	L	h
Specific yield	-	S_y
Porosity	-	n

337

338 3.2. Agronomic Module

339 The agronomic module quantifies the impact of deficit irrigation on actual crop yield. It is important to
 340 account for changes in crop drought sensitivity throughout the growing season (Srinivasa Prasad et al.,
 341 2006). Therefore, the agronomic module uses growth stage specific crop production functions that relate
 342 relative evapotranspiration rate (ET_{act}/ET_p) to relative crop yield (Y_a/Y_m). Raes et al. (2005) summarized
 343 various ways of modeling the relation between relative crop ET and relative crop yield. Based on the
 344 available methods, Eq. 2 was selected because this method accounts for changes in the relation and
 345 effects of deficit irrigation at different crop growth stages, and is appropriate for the monthly time-scale
 346 of our model.

$$347 \frac{Y_a}{Y_m} = \prod_{i=1}^N (1 - k_{y,i} (1 - \frac{ET_{act,i}}{ET_{p,i}})) \quad (2)$$

348 where Y_a and Y_m are actual and potential crop yield (kg/ha) (Table S3), N is total number of crop growth
 349 stages ($N=4$ for wheat, maize, tomato, canola, and sorghum and $N=1$ for sugar beet, alfalfa, and saffron)
 350 (see Fig. S1), $k_{y,i}$ is yield response factor for crop growth stage i (see Fig. S1), $ET_{act,i}$ is actual crop
 351 evapotranspiration for crop growth stage i , and $ET_{p,i}$ is potential crop evapotranspiration for crop growth

352 stage i . Actual and potential crop evapotranspiration are calculated in the hydrologic module using the
 353 following equations:

$$ET_p = k_c (PET) \quad (3)$$

$$ET_{act} = ET_p \left(\frac{5z - 2z^2}{3} \right) \quad (4)$$

355 where PET is reference evapotranspiration based on Penman-Monteith (Allen et al., 1998), k_c is growth
 356 stage specific crop coefficient (Table S2), and z is relative soil water content (Table 2). Relative soil water
 357 content (z) is equal to the pore volume fraction filled with water. Values of z can range from 0 (dry) to 1
 358 (saturated). The value of z in this equation is simulated by the hydrologic module as detailed in
 359 Dehghanipour et al. (2019). Eqs. (4) and (2) show that crop yield is directly related to relative soil water
 360 content z . Therefore, deficit irrigation reduces relative soil water content, which reduces actual crop
 361 evapotranspiration and consequently crop production.

362 3.3. Economic Module

363 The economic module calculates the net profit of crop production using the following equation:

$$Profit = \sum_u \sum_{cr} A_{u,cr} (Y_{a_{u,cr}} P_{cr} - C_{cr}) - \sum_u DC_u \quad (5)$$

365 where u is the number of agricultural zones (i.e. 21), cr is a crop index (going from 1 to 5 or 8 for the
 366 current and proposed crop pattern, respectively), $A_{u,cr}$ is crop acreage for crop cr in agricultural zone u
 367 [ha], $Y_{a_{u,cr}}$ is actual crop yield for crop cr in agricultural zone u [Kg/ha], P_{cr} is price for crop cr
 368 [USD/Kg], C_{cr} is production cost for crop cr excluding maintenance and water delivery costs [USD/ha],
 369 and DC_u is maintenance and water delivery costs in agricultural zone u [USD]. The actual crop yield is
 370 calculated in the agronomic module using Eq. (2). Crop prices and production costs are specified as input
 371 parameters to the model (Table S3). Maintenance and water delivery costs are equal to 3% of total gross
 372 profit ($\sum_u \sum_{cr} A_{u,cr} (Y_{a_{u,cr}} P_{cr})$), which farmers pay to the Ministry of Energy of Iran.

373

374 3.4. Objective Functions

375 We formulate an optimization problem with two objective functions, i.e. an agricultural index (F_1)
 376 quantifying net agricultural profit in the Miyandoab Plain, and an environmental index (F_2) quantifying
 377 the degree to which environmental flow requirements to Lake Urmia are met. There is an inherent trade-
 378 off between these two objectives, since maximizing profit (F_1) will tend to withdraw more surface water
 379 for irrigation, leading to decreased environmental flow (F_2) toward downstream Lake Urmia (Fig. 1).
 380 Two versions of the agricultural index are considered, one focusing on long-term economic profit
 381 (economic agricultural index, F_1), and the other focusing on long-term sustainability (sustainable
 382 agricultural index, F_1^*). The economic agricultural index is based on long-term net agricultural profit:

$$F_1 : \text{Economic agricultural index} = \frac{1}{n} \sum_y \left(\frac{Profit_y}{Profit_{Historical}} \right) \quad (6)$$

383

384 where n is the number of years simulated ($=30$), y represents a year in the simulation period (1984-2013),
 385 $Profit_y$ is net profit in year y , and $Profit_{Historical}$ is the historical average net annual profit over the period
 386 1984-2013. $Profit_y$ is calculated by the Economic module. We did not have statistical data for the time
 387 series of historical profit and used the simulation model to calculate historical profit. We used available
 388 statistical data (for crop acreage, crop pattern, groundwater pumping, and irrigation method) and consider
 389 some constraints (for irrigation canals, groundwater pumping, and Bukan reservoir) in the simulation
 390 model for calculating the time series of historical profit.

391 Including historical profits in the objective function provides a useful benchmark: a value equal to 1 for
 392 the economic agricultural index indicates a scenario, in which long-term agricultural profits are similar to
 393 the historical situation, whereas values greater (smaller) than 1 indicate greater (smaller) profits compared
 394 to the historical situation. This objective function prefers values for the decision variables that maximize
 395 long-term average agricultural profit without consideration for the inter-annual fluctuations in agricultural
 396 profit. For instance, very low profits during droughts are tolerated, as long as this is compensated by high
 397 profits during wet periods.

398 However, such extreme inter-annual variations in profit may not be warranted, and more stable incomes
 399 and profits may be preferred. Therefore, an alternative objective function uses a sustainable agricultural
 400 index, based on a weighted combination of three sustainability indices (Cai et al., 2002; Schoups et al.
 401 2006):

$$402 \quad F_1^*: \text{Sustainable agricultural index} = W_1 \frac{REL}{REL_{Historical}} + W_2 \frac{RES}{RES_{Historical}} + W_3 \frac{IVUL}{IVUL_{Historical}} \quad (7)$$

403 where W_1 , W_2 , W_3 are three weights, REL is net agricultural profit reliability, RES is net agricultural profit
 404 resiliency, and $IVUL$ is net agricultural profit invulnerability. These variables are calculated with the
 405 following equations:

$$REL = \frac{1}{n} \sum_y \frac{Profit_y}{Profit_{Historical}} \quad (8)$$

$$406 \quad RES = 1 - \frac{nfail}{n} \quad (9)$$

$$IVUL = Min \left\{ \frac{Profit_y}{Profit_{Historical}} \right\} \quad (10)$$

407 where $nfail$ is the number of successive years that net agricultural profit is smaller than 90% of
 408 $Profit_{Historical}$. The REL index in the objective function is similar to Eq. (6) and maximizes long-term
 409 agricultural profit. This term is driven by agricultural profits in non-drought (HD1) years (Table 1), when
 410 there is enough water to meet maximum agricultural water demand. The RES index in the objective
 411 function prevents extended periods of lower than (90% of) average agricultural profits. This may happen
 412 during droughts (successive HD2 and HD3 years, Table 1), when decreased water supply limits
 413 agricultural production. We assume 10% as risk threshold, because a reduction in agricultural profit up to

10% has no significant impact on sustainable agricultural profit. Finally, the *IVUL* index prefers decision variables that maximize the smallest agricultural profits over all n years. Smallest profit is expected during the most extreme drought conditions, in this case study this corresponds to moderate drought years (HD3, Table 1), since more extreme drought conditions are not encountered in the historical time series. Therefore the *IVUL* index controls the value of agricultural profits during the HD3 period, when there is severe competition between agricultural and environmental water demands. Hence, via the weighted combination of *REL*, *RES*, *IVUL*, the sustainable agricultural index in Eq. (7) considers agricultural profit in each drought period. To prevent significant reductions in agricultural profits, emphasis is placed here on the *IVUL* index, resulting in values for the weights W_1 , W_2 , and W_3 of 0.25, 0.25, and 0.5, respectively. The environmental objective function is expressed as an environmental index given by the following equation:

$$F_2 : \text{Environmental index} = \frac{1}{n} \sum_y \left(\frac{POI_y \times \text{Penalty term}_y}{POI_{\text{Historical}}} \right) \quad (11)$$

where POI is the fraction of the total of all upstream flow into Miyandoab Plain in year y that flows to Urmia lake, and is calculated by the following equation:

$$POI_y = \frac{\sum (Q_{out})_y}{\sum (Q_{in})_y} \quad (12)$$

where summation in the numerator gives total downstream discharge in all rivers that flow out of the Miyandoab Plain and into Lake Urmia, and summation in the denominator gives total upstream discharge in all rivers that flow into Miyandoab Plain. Downstream river discharge is calculated with the hydrologic module. Quantity Penalty term_y in Eq. (11) is a fraction between 0 and 1 that penalizes failure to meet minimum environmental flow requirements. It is calculated with the following equation:

$$\text{Penalty term}_y = \begin{cases} 1 & (Q_{out,zar})_y \geq (LD_{zar})_y \\ \frac{(Q_{out,zar})_y}{(LD_{zar})_y} & (Q_{out,zar})_y < (LD_{zar})_y \end{cases} \quad (13)$$

where $(Q_{out,zar})_y$ is downstream discharge to Urmia lake of the Zarrineh Rood river in year y , and $(LD_{zar})_y$ is the minimum environmental flow requirement to Urmia lake from Zarrineh Rood in year y . Downstream discharge $(Q_{out,zar})_y$ depends on water releases from Bukan reservoir and is calculated with the hydrologic module, whereas $(LD_{zar})_y$ is treated as a decision variable, as discussed in the next section.

Summarizing, we consider two sets of objective functions: strategy I simultaneously maximizes the economic agricultural index F_1 (Eq. 6) and the environmental index F_2 (Eq. 11), while strategy II simultaneously maximizes the sustainable agricultural index F_1^* (Eq. 7) and the environmental index F_2 (Eq. 11). These multi-objective optimization problems are solved using the Multi-Objective Particle Swarm Optimization (MOPSO) algorithm, which results in quantification of the trade-off Pareto front

444 between the two conflicting objective functions (Coello et al., 2004). More details about MOPSO are
445 presented in Dehghanipour et al. (2019).

446

447 **3.5. Decision Variables**

448 The decision variables for strategies I and II and their lower and upper bounds are listed in Table 3. The
449 decision variables include (1) total crop acreage, (2) threshold relative soil water content to trigger
450 irrigation (“intervention point” z_{int} in Eq. 15), and (3) fraction of inflow to Bukan reservoir allocated for
451 environmental flow. The optimization of complex water resources systems often becomes
452 computationally intractable when solving optimization problems with large numbers of decision variables
453 (Loucks and van Beek, 2005). In this study, to reduce the number of decision variables, we group
454 decision variables by hydrologic drought period based on the SDI. According to Table 1, by using the
455 SDI, the historical period of 30 years (1984-2013) can be divided into periods of non-drought, mild
456 drought, and moderate drought, thus reducing the number of decision variables by a factor of 10 (from 30
457 years to 3 drought periods).

458 Total crop acreage directly affects agricultural profit given crop prices and production costs, and it
459 directly affects water consumption in Miyandoab Plain and inflow to Urmia Lake. Treating total crop
460 acreage as a decision variable permits flexibility in dealing with hydrologic drought conditions and
461 agricultural demand. In strategy I, the lower bound for total crop acreage was 0 and the upper bound was
462 set as the total irrigable area, based on studies of the Ministry of Energy of Iran (2016). Moreover, in
463 strategy I we consider three separate decision variables for total crop acreage, one for each drought period
464 (HD1, HD2, and HD3). In strategy II on the other hand, focus is on sustainability of agricultural profits.
465 In that case, the lower bound for total crop acreage was set equal to the current irrigated area. Moreover,
466 to avoid large fluctuations in acreage, we use one decision variable for total crop acreage for all drought
467 periods.

468 Total crop acreage is distributed over agricultural zones by assuming that each agricultural zone has the
469 same crop pattern:

$$470 \quad A_{y,u,cr} = A_y \frac{MaxA_u}{\sum_u MaxA_u} \alpha_{cr} \quad (14)$$

471 where $A_{y,u,cr}$ is the area of crop cr in agricultural zone u in year y , A_y is total crop acreage in year y , $MaxA_u$
472 is the irrigable area of agricultural zone u , and α_{cr} is contribution of crop cr in the crop pattern (see Fig.
473 3). Our analysis considers both crop patterns in Fig. 3. The advantage of using equation (14) is that it
474 ensures spatial equity among agricultural zones in terms of crop production and opportunity for
475 agricultural profit. Another advantage is that it further reduces the number of decision variables (Schoups
476 et al., 2006).

477 Irrigation demand is a function of relative soil water content so that irrigation begins when relative soil
 478 water content drops below a specified threshold or intervention value, z_{int} , and irrigation continues until
 479 soil water content reaches a specified target value, z_{tar} . Therefore, irrigation demand, namely the sum of
 480 SW and GW withdrawal ($Q_{Isw} + Q_{Igw}$), is calculated as follows:

$$481 \quad Q_{Isw} + Q_{Igw} = nZ_r A (z_{tar} - z_{int}) \quad (15)$$

482 where n is porosity and Z_r is rooting depth (Table 2). Since basin irrigation is used in the Miyandoab
 483 Plain, the value of z_{tar} is set equal to 1. Threshold or intervention point z_{int} is treated as a decision
 484 variable; it directly affects the level of deficit irrigation and thus agricultural water use, water diversion,
 485 and profit. For instance, lower values for z_{int} reduce crop yield and water demand (via Eqs. 2 and 4), and
 486 make more water available for environmental flows. As shown in Fig. S1, the FAO considers four values
 487 of yield response factor (k_y) for four growth stages of wheat, maize, tomato, canola, and sorghum, and one
 488 value of k_y for the entire growing season of sugar beet, alfalfa, and saffron. Therefore, we consider four
 489 distinct intervention points each for wheat, maize, tomato, canola, and sorghum, and one intervention
 490 point each for sugar beet, alfalfa, and saffron. The advantage of using these growth-stage specific
 491 decision variables is that it permits flexibility in deficit irrigation for dealing with water shortage and
 492 changes in the timing of irrigation according to the growth stage of each crop. The upper bound of each
 493 z_{int} decision variable was set equal to 60%, which for the loamy soils in the area corresponds to field
 494 capacity (Schroeder et al., 1994), while the lower bound of each z_{int} decision variable was set to 30%,
 495 which is between wilting point (22%) and field capacity (60%).

496 The final decision variable relates to environmental flow releases to Urmia Lake from Bukan reservoir
 497 located on the Zarrineh Rood river. Specifically, we use the fraction MFR of inflow into Bukan reservoir
 498 that is released as environmental flow as a decision variable:

$$499 \quad MFR = \frac{(LD_{zar})_{y,m}}{(Q_{in,zar})_{y,m}} \quad (16)$$

500 where $(LD_{zar})_{y,m}$ is the minimum environmental flow requirement for Urmia lake from Zarrineh Rood
 501 river in year y in month m , and $(Q_{in,zar})_{y,m}$ is the upstream flow of Zarrineh Rood river into Bukan
 502 reservoir in year y and month m . Lower and upper bounds of MFR are taken as 0.2 and 0.85, respectively
 503 (Yasi and Ashori, 2017).

504 In strategy I, we consider one single decision variable for MFR that is constant over the entire period; this
 505 choice is expected to reduce large fluctuations in environmental flow to Urmia Lake, and thus result in a
 506 temporally stable environmental index. As mentioned above, three decision variables are considered for
 507 total crop acreage in strategy I. This degree of freedom allows total crop acreage to be modified to meet
 508 minimum environmental flow requirements. In contrast, in strategy II, we consider three decision
 509 variables for MFR for each drought period (HD1, HD2, and HD3), but one single decision variable for

510 total crop acreage for the entire period. This promotes temporal stability in agricultural profits, with
511 additional flexibility in *MFR* to meet agricultural and environmental water demand.
512 Finally, an important constraint relates to the monthly timing of agricultural and environmental water
513 demand. Fig. 6 shows monthly time-averaged inflow to Bukan reservoir (upstream flow of Zarrineh Rood
514 river) together with monthly potential evapotranspiration (ET_p). Following Eq. 16, environmental flow is
515 allocated proportional to inflow into Bukan reservoir, which mostly occurs from early winter to mid-
516 spring. Therefore, the value of *MFR* has the most significant effect on water storage in Bukan reservoir
517 from early winter to mid-spring, because by increasing *MFR*, more water will be allocated to the lake in
518 this period and less water storage will remain in the reservoir to meet agricultural demand in the spring
519 and summer. On the other hand, the total crop acreage and deficit irrigation (intervention point) decision
520 variables have the most significant effect on water storage in Bukan reservoir from early spring to end of
521 summer, since these variables play a crucial role in agricultural water consumption.

522 **Table 3: Decision variables for the two sets of objective functions in section 3.4**

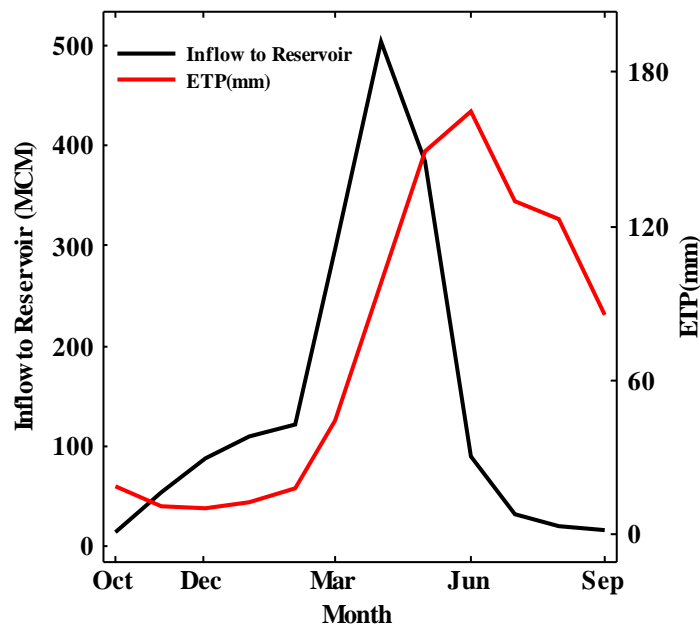
523

Strategy	Objective Functions	Decision Variable ^a	Lower Bound	Upper Bound	Units ^b	Number of Variables ^c
I	(F ₁ , F ₂)	A_y	0	76700	ha	np
		$Zint_{y,cr,s}$	30%	60%	-	$\sum_{ncrop} np \times ns_{ncrop}$
		<i>MFR</i>	20%	85%	-	1
II	(F ₁ [*] , F ₂)	A_y	54200	76700	ha	1
		$Zint_{y,cr,s}$	30%	60%	-	$\sum_{ncrop} np \times ns_{ncrop}$
		<i>MFR</i>	20%	85%	-	np

524 ^a A_y : Total crop acreage in year y , $Zint_{y,cr,s}$: threshold soil moisture content in year y for crop cr in growth stage s , *MFR*: Minimum flow requirement
525 to Urmia lake from the Zarrineh Rood river

526 ^b ha=hectare, 10^4 m²

527 ^c np is number of distinct hydrologic drought periods (=3), $ncrop$ is number of crops (5 in current crop pattern and 8 in proposed crop pattern), ns is
528 number of crop growth stages (4 for wheat, maize, tomato, canola, and sorghum, and 1 for sugar beet, alfalfa, and saffron).
529



530

Fig. 6: Monthly time-averaged inflow to Bukan reservoir (i.e, upstream discharge of Zarrineh Rood river) (MCM) and potential evapotranspiration (ETp) (mm) in Miyandoab Plain

3.6. Variable Constraints

Three sets of variable constraints are used to ensure realism of the optimization results. The first set of constraints limits GW pumping in each agriculture zone to the monthly GW pumping capacity of the zone:

$$Pump_{m,u} \leq PumpCap_u \quad (17)$$

where $Pump_{m,u}$ is GW extraction in agricultural zone u in month m [L^3/T], and $PumpCap_u$ is GW pumping capacity in agricultural zone u [L^3/T]. In this study, the sum of the historically measured maximum monthly pumping rate of wells in each agricultural zone was considered as the monthly pumping capacity for each agriculture zone. This constraint ensures that the optimal solution reflects realistic maximum pumping rates.

SW diversions from the Zarrineh Rood river are conveyed to the primary irrigation canals. Each irrigation canal has a diversion capacity based on its dimensions.

$$Q_{m,c} \leq MaxQ_c \quad (18)$$

where $Q_{m,c}$ is SW diversion to canal c in month m [L^3/T], and $MaxQ_{m,c}$ is diversion capacity of canal c [L^3/T]. This constraint ensures that total monthly SW diversions do not exceed canal conveyance capacities.

Finally, constraints are placed on monthly water storage $S_{y,t}$ in Bukan reservoir:

$$S_{dead} \leq S_{y,t} \leq S_{max} \quad (19)$$

where S_{dead} is dead storage volume of the reservoir and S_{max} is maximum volume of the reservoir. These constraints prevent water releases from dead storage, and allow for releases larger than total water demand (sum of agricultural, urban, and environmental water demand) when the reservoir is full and overtopping occurs.

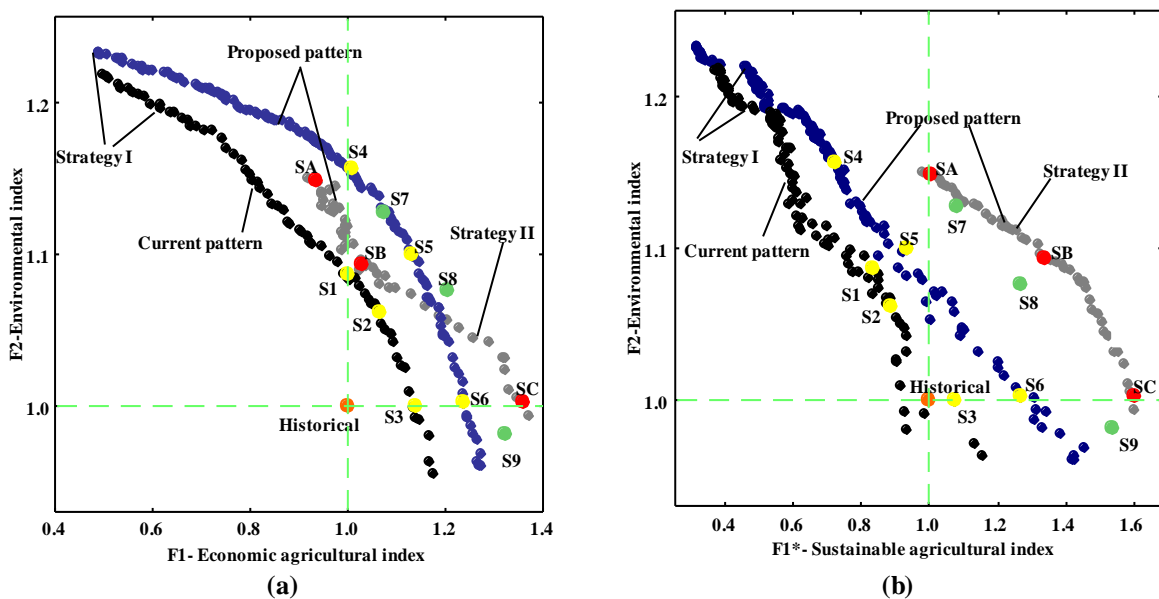
4. Results and discussion

4.1. Water management scenarios for current and proposed crop patterns in strategy I

The Pareto fronts for current and proposed crop patterns in strategy I, i.e., the set of non-dominated simulations that were obtained with the integrated SO water management model, are presented in Figure 7.a. In Fig. 7.a, objective function 2 (Environmental index) is plotted against objective function 1 (Economic agricultural index), and dark and blue nodes indicate the Pareto fronts for current and

566 proposed crop patterns, respectively. The Pareto front consists of many solutions and presents potential
 567 compromises between contradicting objectives. In this study, six scenarios that indicate specific optimal
 568 solutions on the Pareto fronts for strategy I were selected for detailed analysis. These scenarios include
 569 scenarios 1 to 6, as shown by the yellow nodes in Fig. 7.a. Furthermore, the orange node represents values
 570 for the objective functions corresponding to historical water management, which serves as a benchmark.
 571 Scenarios 1 and 4 represent environmental scenarios characterized by an increase in Environmental index
 572 without a change in Economic agricultural index compared to historical conditions. Likewise, scenarios 3
 573 and 6 are economic scenarios with an increase in the Economic agricultural index without a change in
 574 Environmental index compared to historical conditions. Finally, scenarios 2 and 5 represent win-win
 575 situations where both Environmental and Economic agricultural indices are increased compared to
 576 historical conditions.

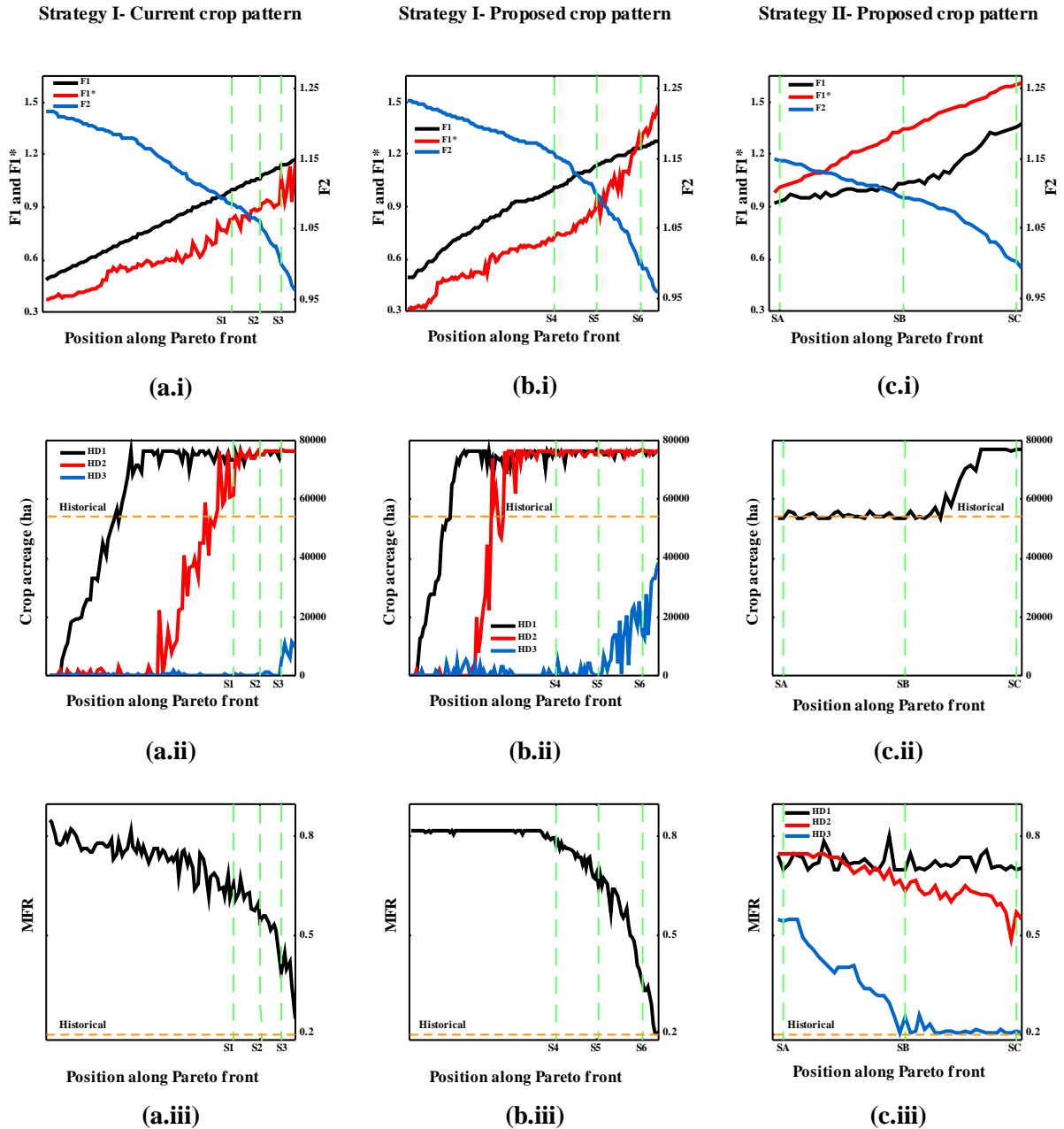
577 In scenario 1, changes in water management (deficit irrigation, changes in crop acreage, and
 578 environmental flow requirement) with the current crop pattern make it possible to increase the
 579 Environmental index by 9% without decreasing the Economic agricultural index. However, increasing the
 580 Environmental index by more than 9% leads to significant reductions in Economic agricultural index.
 581 Likewise, changes in water management with the current crop pattern in scenario 3 increase the
 582 Economic agricultural index by 14% without decreasing the Environmental index, with further increases
 583 in Economic agricultural index requiring significant reductions in the Environmental index.
 584 Similar trade-offs are present in the Pareto front for the proposed crop pattern (Fig. 7a), but at larger
 585 values for both objective functions, thereby clearly demonstrating benefits of the proposed crop pattern on
 586 both the agricultural economy and the environment. For example, scenario 4 increases the Environmental
 587 index by 16% (up from 9% in scenario 1), while scenario 6 increases the Economic agricultural index by
 588 24% (up from 14% in scenario 3).

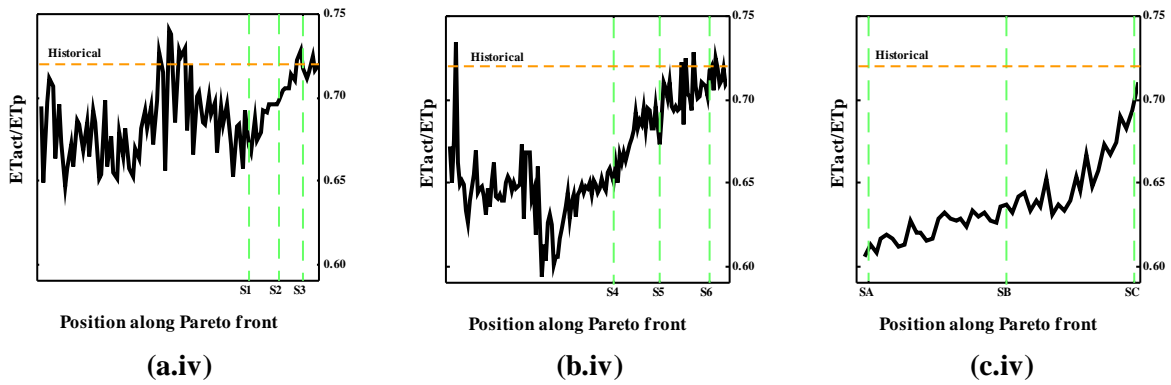


589

590
591
592
593
594
595
596
597
598
599

Fig. 7: Pareto fronts for the multi-objective optimization after 5000 model simulations with the MOPSO algorithm for strategy I and II: (a) Environmental index vs Economic agricultural index, and (b) Environmental index vs Sustainable agricultural index. Black and blue nodes indicate Pareto fronts for current and proposed crop patterns in strategy I (section 4.1), while gray nodes indicate the Pareto front for the proposed crop pattern in strategy II (section 4.3). The orange node represents historical conditions and is used as reference. Selected points on the trade-off curves (“scenarios”) are indicated by yellow and red nodes and are discussed in more detail in the text. The green nodes are simulation scenarios showing the effect of increased GW capacity (S4 moves to S7, S5 moves to S8, S6 moves to S9) as discussed in section 4.2.





600 **Fig. 8: Changes in values for the objective functions and decision variables when moving along the Pareto fronts from**
 601 **left (focus on environment) to right (focus on agriculture). Each column shows a different Pareto front: (a) strategy I**
 602 **with current crop pattern, (b) strategy I with proposed crop pattern, and (c) strategy II with proposed crop pattern.**
 603 **Each row shows a different variable: (i) objective functions, (ii) crop acreage, (iii) minimum environmental flow**
 604 **requirement MFR, and (iv) ratio of actual to potential crop ET (a measure of deficit irrigation). HD1, HD2, HD3 are**
 605 **hydrologic drought conditions defined in Table 1.**
 606

607 Figure 8 provides more detailed insight into how optimal water management changes as one moves along
 608 each of the Pareto fronts in Fig. 7. Moving from left to right along each Pareto front changes the focus
 609 from the environment to agriculture. In strategy I (columns a and b in Fig. 8), the resulting increase in
 610 Economic agricultural index (row i in Fig. 8) is achieved by increasing crop acreage (row ii), decreasing
 611 environmental flow requirement (row iii), and decreasing deficit irrigation (row iv).

612 When moving along the Pareto front, crop acreage in non-drought years (HD1) increases first, followed
 613 by an increase in crop acreage in mild-drought years (HD2). Significantly, crop acreage in moderate-
 614 drought years (HD3) remains near zero along most of the Pareto front, and only starts to increase on the
 615 far-right end of the strategy I Pareto curves, when the environment is all but ignored. This increase is
 616 more pronounced with the proposed than with the current crop pattern (compare Fig. 8.a.ii and 8.b.ii),
 617 because of the lower water requirements of the proposed crop pattern (Table S4 and Table S5). These
 618 results indicate that, even though strategy I results in better water management with benefits for both the
 619 environment and agriculture, it does not protect agriculture against short-term effects of moderate to
 620 severe droughts. This is also clear in Fig. 7b, where the strategy I Pareto scenarios do not score that well
 621 on the Sustainable agricultural index. More sustainable management strategies may therefore be required
 622 (see sections 4.2 and 4.3).

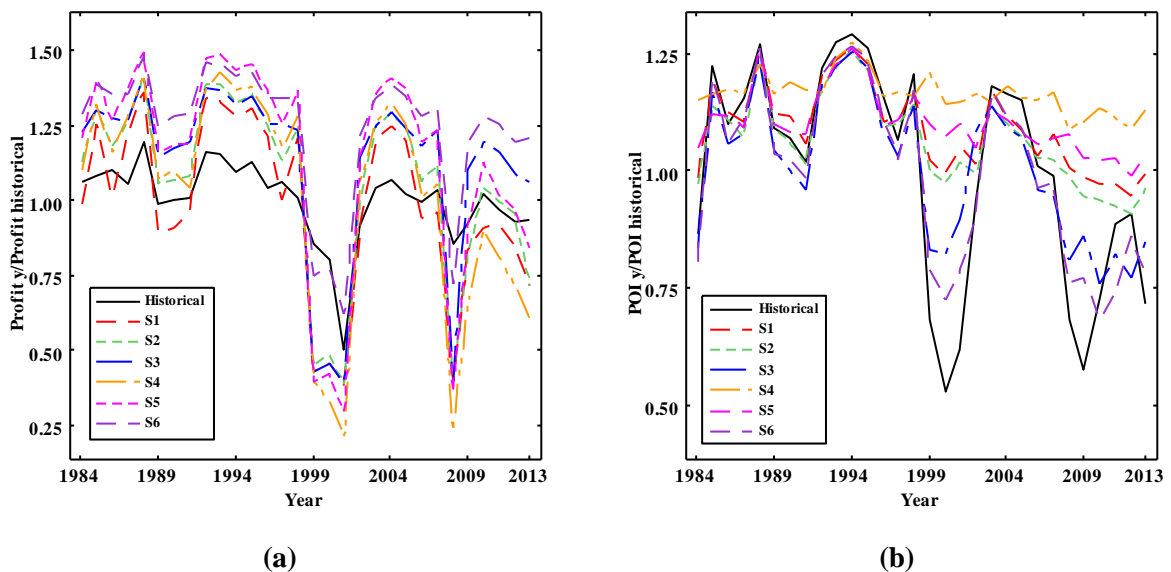
623 Once crop acreages are at their maximum level, further increases in the Economic agricultural index are
 624 achieved by reducing environmental flow requirement (Fig. 8.a.iii and 8.b.iii), which reallocates water to
 625 agriculture, and reducing deficit irrigation (Figs. 8a.iv, 8.b.iv, and S3). These effects are visible when
 626 moving from scenario 1 to scenario 3 (column a in Fig. 8), and similarly when moving from scenario 4 to
 627 scenario 6 (column b in Fig. 8).

628 The dynamics of annual agricultural profit (relative to historical) for six Pareto scenarios are shown in
 629 Fig. 9a. In non-drought (HD1) years and pre-2008 mild-drought (HD2) years (1984, 1986, 1989, 1990,

1991, 1997, 2002, 2006, 2007), agricultural profits for all scenarios are equal or higher than historical profits (Fig. 9.a), because of the larger total crop acreages for those years compared to historical ($A_{historical}=54200$ ha).

In post-2008 HD2 years (2009-2013), agricultural profit is less than historical in the environmental scenarios (scenarios 1 and 4) and the win-win scenarios (scenarios 2 and 5). The reason for this is greater water allocation to the environment (larger MFR) in those years compared to historical, resulting in deficit irrigation and crop water stress. Finally, in the moderate-drought (HD3) years (1999-2001, and 2008), all scenarios, with the exception of scenario 6, exhibit a sharp decrease in agricultural profit, due to near-zero crop acreages in those years, with agricultural production limited to orchards. This confirms the lower scores of these scenarios on the Sustainable agricultural index, as already seen in Fig. 7b.

Figure 9.b shows dynamics of annual inflow to Lake Urmia relative to historical conditions. As mentioned before, the MFR and crop acreage of the six scenarios in HD1 and HD2 years are higher than historical ($MFR_{historical}=0.2$ and $A_{historical}=54200$ ha), which increases environmental flow requirement and agricultural demand compared to historical conditions. In HD3 years, inflow to Lake Urmia is more stable in the six Pareto scenarios compared to historical. This is in line with lower crop acreages in those years (Fig. 9a), less irrigation water withdrawals, and thus relatively more water available for the environment.



646 **Fig. 9: Time series of (a) annual agricultural profit and (b) inflow to Lake Urmia expressed as POI in Eq. 12 (both**
 647 **relative to average historical conditions) for six Pareto scenarios of strategy I (S1-S3 use the current crop pattern, S4-S6**
 648 **use the proposed crop pattern).**
 649

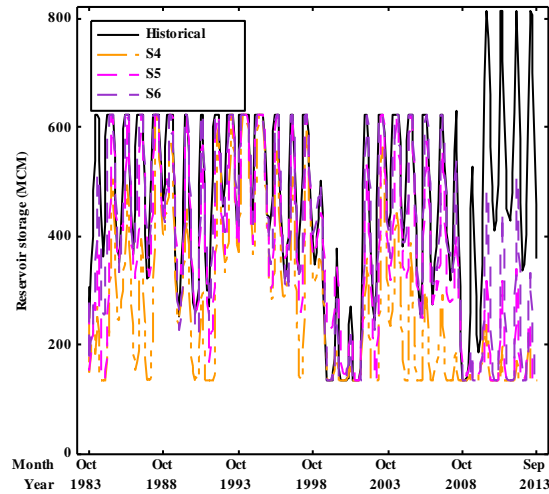


Fig. 10: Time series of monthly Bukan reservoir storage for three Pareto scenarios of strategy I with the proposed crop pattern.

650
651
652
653

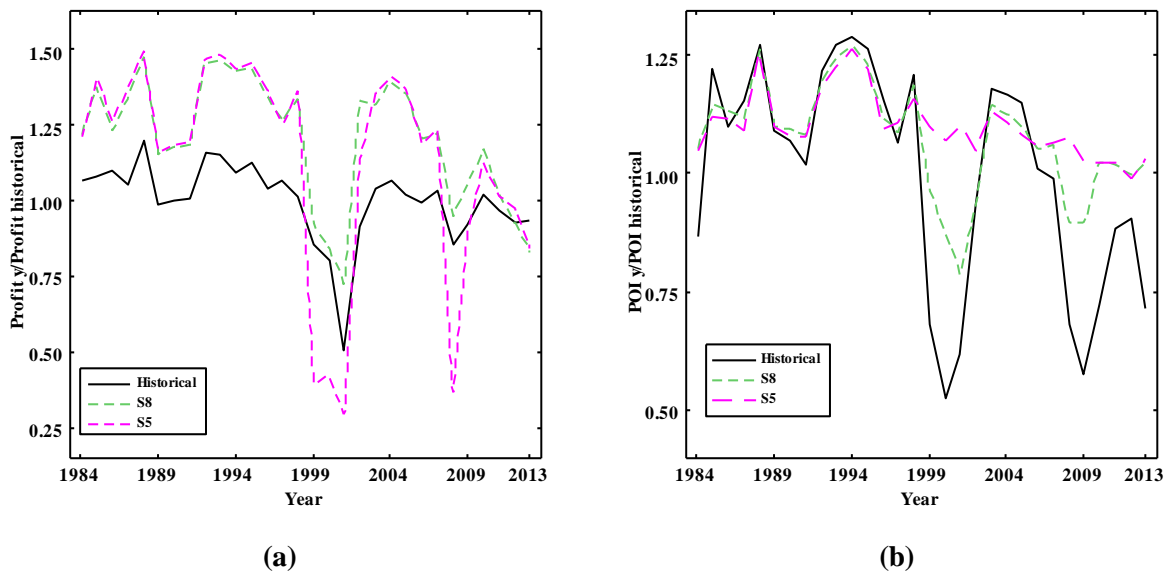
654 Next, Fig. 10 shows dynamics of water storage in Bukan reservoir. More water is stored in scenarios that
655 focus on irrigation (e.g. S6), due to the delay between reservoir inflow and crop water demand, as shown
656 in Fig. 6. In 2008, dam height and storage capacity of Bukan reservoir was increased from 650 to 808
657 MCM, as clearly visible in Fig. 10. The purpose of this increase was to ensure sufficient water supply to
658 nearby cities in extreme droughts. Historically, the increased capacity has led to more water being stored
659 in the reservoir after 2008 (Fig. 10), resulting in relatively less water allocation to agriculture and Lake
660 Urmia. All scenarios in Fig. 10 show that storing less and releasing more water leads to greater benefits.

661 Finally, the water management model also provides insights into the effects of water management on the
662 root-zone water balance in the region (Table S4 and Table S5). As expected, GW pumping, SW
663 withdrawal, and actual crop ET all increase from scenario 1 to 3 (and from scenario 4 to 6), which
664 correspond to increasing Economic agricultural index and decreasing Environmental index. Increases in
665 actual crop ET reflect decreases in deficit irrigation, i.e. more water available for irrigation and less for
666 environmental flow to the lake.

667 Note that SW withdrawal, GW pumping, and actual crop ET in the proposed-crop-pattern scenarios (4, 5,
668 and 6) are lower than the corresponding current-crop-pattern scenarios (1, 2, and 3), due to the lower
669 water requirements for the proposed crop pattern.

670 **4.2. Increasing GW pumping capacity: a simulation analysis of strategy I scenarios**
671 The previous section illustrated that water management based on strategy I scenarios results in sharp
672 decreases in agricultural profit during droughts (Fig. 9). Even though groundwater is in principle
673 available to deal with such shocks, current pumping capacity limits greater reliance on groundwater
674 during droughts. This section investigates to what extent an increase in GW pumping capacity can
675 improve agricultural sustainability during droughts without compromising GW level stability. To this
676 end, scenarios S4-S6 (proposed crop pattern) are taken as starting point, and are modified into three new

677 scenarios (S7-S9). The modifications are detailed in Table S6, and basically correspond to changing crop
678 acreage and GW pumping capacity in the model during the dry HD3 years: crop acreage is set equal to
679 the historical acreage (about 75% of the maximum area), while GW pumping capacity is doubled.
680 The model is then run with these new inputs (i.e., a simulation is done, not an optimization), and the
681 resulting values of the objective functions are shown in Fig. 7. We see that scenarios 7, 8, and 9 result in
682 greater values for the Economic agricultural index, but smaller values for the Environmental index,
683 compared to the corresponding scenarios 4, 5, and 6 (Fig. 7a). Furthermore, the effect on the Sustainable
684 agricultural index is significant (Fig. 7b), suggesting greater agricultural sustainability of these new
685 scenarios that use an increased GW pumping capacity. These observations are confirmed by the time-
686 series in Fig. 11, which show increased agricultural profits during droughts, but also decreases in
687 environmental flows to the lake. This indicates that the doubled GW pumping capacity used in these new
688 scenarios is not sufficient to support the targeted crop acreages without reallocating additional surface
689 water from the environment to agriculture.
690 The effects of increased GW pumping on the water balance and on groundwater levels are shown in Figs.
691 S4 and 12. Drops in groundwater level are most pronounced in scenario 7 (Fig. 12), which, out of the
692 three new scenarios, is characterized by the largest SW allocation to the lake, the smallest SW extraction
693 for irrigation, largest fraction of GW use for irrigation, and the smallest GW recharge (Fig. S4).



694 **Fig. 11: Time series of (a) annual agricultural profit, and (b) inflow into lake Urmia expressed as POI in Eq. 12, for**
695 **scenario 5 (original GW pumping capacity) and scenario 8 (doubled GW pumping capacity).**
696
697

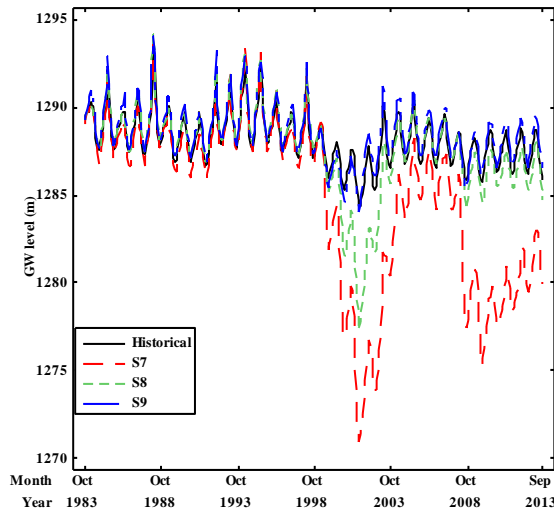


Fig. 12: Time-series of monthly GW level for increased GW pumping capacity scenarios 7 to 9.

698
699
700

701 4.3. Water management scenarios for proposed crop pattern in strategy II

702 In addition to simulation as used in section 4.2, sustainable water management options can also be
 703 explored by directly optimizing the Sustainable agricultural index. These strategy II results are presented
 704 in this section. The resulting Pareto front for proposed crop pattern in strategy II is shown in Fig. 7 with
 705 gray nodes. We focus on three specific Pareto scenarios A, B, and C shown in red in Fig. 7. These
 706 scenarios show that it is possible to, compared to historical conditions, (1) increase the Environmental
 707 index without any decrease in the Sustainable agricultural index (scenario A), (2) increase the Sustainable
 708 agricultural index without a change in the Environmental index (scenario C), and (3) increase both the
 709 Environmental and Sustainable agricultural index at the same time (scenario B).

710 The third column in Fig. 8 shows how optimal water management changes along the Pareto front of
 711 strategy II. The value of the Sustainable agricultural index increases when moving across the Pareto front
 712 from left to right. In the first half of the Pareto front, this increase is achieved, not by increasing crop
 713 acreage, which remains constant initially, but by decreasing the environmental flow requirement (*MFR*)
 714 during moderate droughts (HD3), which has the effect of reallocating SW from the environment to
 715 agriculture. It is only in the second half of the Pareto front that further increases in the Sustainable
 716 agricultural index are achieved by increasing crop acreage and decreasing deficit irrigation (Fig. 8.c.iv
 717 and Fig. S5).

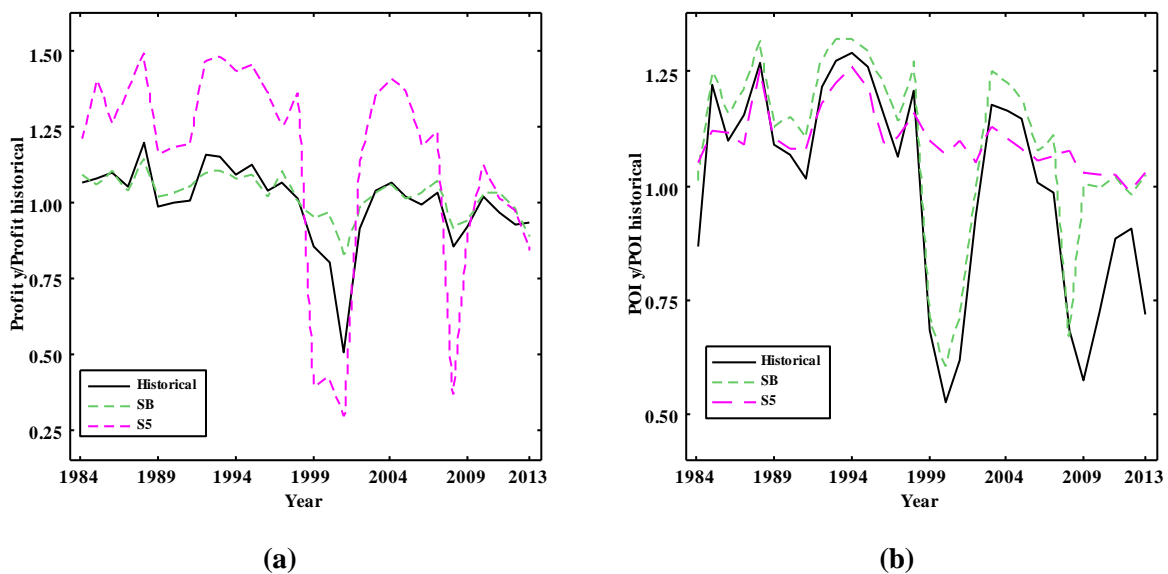
718 As shown in Fig. 8.c.iii, the environmental flow requirement (*MFR*) in the HD1 years is constant and
 719 close to the maximum level, while *MFR* in the HD2 years decreases only slightly. This indicates that the
 720 environmental flow requirement of the lake is met in the HD1 and HD2 years (non- and mild-droughts).
 721 Hence, the trade-off in water allocation between the environment and agriculture only really comes into
 722 play during moderate droughts (HD3 years), as shown by the decrease in *MFR* during HD3 years in Fig.
 723 8.c.iii: temporarily reducing water allocations to the environment during moderate-droughts benefits
 724 agricultural production and sustainability. Such a strategy is illustrated by scenario SB in Fig. 13: sharp

725 decreases in agricultural profit during droughts are prevented at the expense of temporary decreases in
 726 environmental flow to the lake. Such a strategy could make sense as long as it results in short-term
 727 decreases in lake water level that fully recover during the next non-drought period, thereby avoiding any
 728 long-term downward trend in lake water level.

729 In terms of agricultural profit, there is also a trade-off between maximizing net agricultural profit, as done
 730 in strategy I, and preventing significant decreases in profit during droughts. This becomes clear by
 731 plotting the Pareto front of strategy II in Fig. 7.a next to the Pareto front of strategy I: the Economic
 732 agricultural index for scenarios A and B is less than for scenarios 4 and 5, due to lower crop acreages in
 733 the former. However, crop acreage of scenario C is equal (HD1, HD2) or larger (HD3) than crop acreage
 734 of scenario 6, making scenario C superior for both Economic and Sustainable agricultural indices. On the
 735 other hand, scenario C does not score well on the Environmental index.

736 Fig. S6 shows the monthly time series of the Bukan storage reservoir for scenarios A, B, and C of strategy
 737 II. The maximum storage volumes for all scenarios are less than 650 MCM. As mentioned before, this
 738 result indicates that increasing the storage capacity of the reservoir after 2008 does not contribute to
 739 higher values for the objective functions. Finally, Fig. S7 shows time series of monthly GW levels, which
 740 are similar to historical conditions.

741



742 **Fig. 13: Time series of (a) annual agricultural profit and, (b) annual inflow to lake Urmia expressed as POI in Eq. 12,**
 743 **for the win-win Pareto scenarios of strategy I (S5) and strategy II (SB).**
 744

745 In this study, we tried to reduce uncertainty in the development of the simulation-optimization model. For
 746 instance, all input data come from government agencies in Iran that have established data quality control
 747 procedures. Furthermore, we used multi-objective calibration for the hydrologic module. The advantage
 748 of multi-objective calibration with both river discharge data and groundwater level data (two independent
 749 datasets) is that we can identify any inconsistencies in the model and/or the data. The absence of

750 significant trade-offs in fitting these two observation datasets in the multi-objective calibration of the
751 hydrologic model provides some confidence in the outputs of the hydrological model for the water
752 balance component (Dehghanipour et al., 2019). However, we believe that more research is required to
753 quantify and consider uncertainty in the development of the simulation-optimization model. For example,
754 future climate change , will lead to changes in climatic variables, e.g., temperature, precipitation, snow,
755 and evapotranspiration, that in turn result in changes in river runoff and surface water availability.
756 Therefore, climate change is causing uncertainty in the inflow to reservoirs and related planning (Hakami-
757 Kermani et al., 2020). Consequently, future work will focus on assessing the effects of climate change
758 uncertainty on the planning and management of water resources to meet agricultural water demand in
759 Miyandoab plain and environmental flow requirements of Urmia Lake.

760 **5. Conclusions**

761 The paper has presented and applied a simulation-optimization (SO) approach for identifying water
762 management strategies in irrigated endorheic river basins that ensure sustainability of irrigated agriculture
763 while meeting downstream environmental flow requirements. Our analysis contributes both novel
764 methodology and novel insights into water management in the application case study.

765 In terms of methodology; first, the issue of estimating minimum environmental flow requirements is
766 tackled by including it as a decision variable in the optimization model, which adds more flexibility
767 compared to existing approaches that either include it as a precomputed constraint or as an objective to be
768 maximized. Second, the hydrologic simulation model in our SO approach includes both SW and GW
769 components in the form of dynamically coupled WEAP and MODFLOW models. As such, the
770 optimization model searches a larger solution space that includes conjunctive use as a potential long-term
771 strategy. Finally, multi-objective optimization is used to yield an entire Pareto set of water management
772 strategies that quantify the trade-off between meeting environmental water demand, quantified by an
773 environmental flow objective function, and meeting agricultural water demand, quantified by either a
774 maximum or sustainable profit objective function.

775 The methodology was applied to the irrigated Miyandoab Plain, a strategic agricultural region in the
776 semi-arid and endorheic Lake Urmia basin, located in the northwest of Iran. There is direct competition
777 between environmental flow requirements tot sustain water levels of Lake Urmia and upstream irrigation
778 withdrawals in the Miyandoab Plain. A recent drought in the region has further increased this competition
779 and led to decreased flow into and continued shrinking of the lake. Results show that a specific
780 combination of minimum environmental flow requirements, deficit irrigation, and cropping patterns can
781 increase environmental flow to Lake Urmia by up to ~16% compared to historical conditions, without
782 decreasing agricultural profits. An alternative combination of these decision variables increases
783 agricultural profits by up to 24% compared to historical conditions, without decreasing environmental

784 flows to the lake. Multiple trade-off options also exist in between these two extremes that simultaneously
785 increase the environmental and agricultural objectives compared to historical conditions. A disadvantage
786 of strategies that maximize long-term agricultural profit is that they result in significant drops in
787 agricultural profit during droughts. An alternative multi-objective optimization was therefore considered
788 which replaced the agricultural profit-maximizing objective with an objective function that emphasizes
789 sustainability of agricultural profits. This analysis revealed that drops in agricultural profit during
790 droughts can be avoided by increasing agricultural GW pumping capacity and temporarily reducing the
791 lake's minimum environmental flow requirements. This may be an attractive strategy during droughts that
792 are neither too long or too severe, so that resulting declines in groundwater and lake water levels are
793 temporary and fully recover after the drought. Overall, the application highlights the feasibility and
794 flexibility of the proposed approach in identifying a range of potential water management strategies in a
795 complex agricultural endorheic basin like the Lake Urmia basin.

796

797 **Competing interests**

798 The authors declare no competing interests.

799

800 **Funding source**

801 This research did not receive any specific grant from funding agencies in the public, commercial, or not-
802 for-profit sectors.

803 **Acknowledgment**

804 We are grateful to the Ministry of Energy of Iran, Urmia Lake Restoration Program (ULRP), and I.R. of
805 Iran Meteorological Organization (IRIMO) for providing the primary data for this research study.
806 We appreciate valuable help from experts of the department of water resources in Yekom Consulting
807 Engineers Company (<http://www.yekom.com/>).

808 **Reference**

- 809 Ahmadzadeh, H., Morid, S., Delavar, M., Srinivasan, R., 2016. Using the SWAT model to assess the
810 impacts of changing irrigation from surface to pressurized systems on water productivity and water
811 saving in the Zarrineh Rud catchment. *Agric. Water Manag.* 175, 15–28.
812 <https://doi.org/10.1016/j.agwat.2015.10.026>
- 813 Allen, R.G., Pereira, L.S., Raes, D., Smith, M., 1998. FAO Irrigation and drainage paper No. 56. Rome:
814 Food and Agriculture Organization of the United Nations.
- 815 Anghileri, D., Castelletti, A., Pianosi, F., Soncini-Sessa, R., Weber, E., 2013. Optimizing watershed
816 management by coordinated operation of storing facilities. *J. Water Resour. Plan. Manag.* 139, 492–
817 500. [https://doi.org/10.1061/\(ASCE\)WR.1943-5452.0000313](https://doi.org/10.1061/(ASCE)WR.1943-5452.0000313)
- 818 Arthington, A.H., Bhaduri, A., Bunn, S.E., Jackson, S.E., Tharme, R.E., Tickner, D., Young, B.,
819 Acreman, M., Baker, N., Capon, S., Horne, A.C., Kendy, E., McClain, M.E., Poff, N.L., Richter,
820 B.D., Ward, S., 2018. The Brisbane Declaration and Global Action Agenda on Environmental Flows
821 (2018). *Front. Environ. Sci.* 6. <https://doi.org/10.3389/fenvs.2018.00045>

- 822 Bai, J., Chen, X., Li, J., Yang, L., Fang, H., 2011. Changes in the area of inland lakes in arid regions of
823 central Asia during the past 30 years. *Environ. Monit. Assess.* 178, 247–256.
824 <https://doi.org/10.1007/s10661-010-1686-y>
- 825 Bai, J., Chen, X., Yang, L., Fang, H., 2012. Monitoring variations of inland lakes in the arid region of
826 Central Asia. *Front. Earth Sci.* 6, 147–156. <https://doi.org/10.1007/s11707-012-0316-0>
- 827 Barbier, E.B., Koch, E.W., Silliman, B.R., Hacker, S.D., Wolanski, E., Primavera, J., Granek, E.F.,
828 Polasky, S., Aswani, S., Cramer, L.A., Stoms, D.M., 2009. Coastal ecosystem-based management
829 with nonlinear in ecological functions and values. *Zhongguo Renkou Ziyuan Yu Huan Jing/ China*
830 *Popul. Resour. Environ.* 19, 125–128. <https://doi.org/10.1126/science.1150349>
- 831 Cai, X., McKinney, D.C., Lasdon, L.S., 2002. A framework for sustainability analysis in water resources
832 management and application to the Syr Darya Basin. *Water Resour. Res.* 38, 21-1-21–14.
833 <https://doi.org/10.1029/2001wr000214>
- 834 Cai, X., Rosegrant, M.W., 2004. Optional water development strategies for the Yellow River Basin:
835 Balancing agricultural and ecological water demands. *Water Resour. Res.* 40.
836 <https://doi.org/10.1029/2003WR002488>
- 837 Chunyu, X., Huang, F., Xia, Z., Zhang, D., Chen, X., Xie, Y., 2019. Assessing the Ecological Effects of
838 Water Transport to a Lake in Arid Regions: A Case Study of Qingtu Lake in Shiyang River Basin,
839 Northwest China. *Int. J. Environ. Res. Public Health* 16, 145. <https://doi.org/10.3390/ijerph16010145>
- 840 Coello, C.A.C., Pulido, G.T., Lechuga, M.S., 2004. Handling Multiple Objectives With Particle Swarm
841 Optimization. *IEEE Trans. Evol. Comput.* 8, 256–279.
842 <https://doi.org/https://ieeexplore.ieee.org/document/1304847>
- 843 Dehghanipour, A.H., Zahabiyou, B., Schoups, G., Babazadeh, H., 2019. A WEAP-MODFLOW surface
844 water-groundwater model for the irrigated Miyandoab plain, Urmia lake basin, Iran: Multi-objective
845 calibration and quantification of historical drought impacts. *Agric. Water Manag.* 223, 105704.
846 <https://doi.org/10.1016/j.agwat.2019.105704>
- 847 Dunn, S.M., Stalham, M., Chalmers, N., Crabtree, B., 2003. Adjusting irrigation abstraction to minimise
848 the impact on stream flow in the east of Scotland. *J. Environ. Manage.* 68, 95–107.
849 [https://doi.org/10.1016/S0301-4797\(03\)00006-9](https://doi.org/10.1016/S0301-4797(03)00006-9)
- 850 Fallah-Mehdipour, E., Bozorg-Haddad, O., Loáiciga, H.A., 2020. Climate-environment-water: integrated
851 and non-integrated approaches to reservoir operation. *Environ. Monit. Assess.* 192.
852 <https://doi.org/10.1007/s10661-019-8039-2>
- 853 Fallah-Mehdipour, E., Bozorg-Haddad, O., Loáiciga, H.A., 2018. Calculation of multi-objective optimal
854 tradeoffs between environmental flows and hydropower generation. *Environ. Earth Sci.* 77.
855 <https://doi.org/10.1007/s12665-018-7645-6>
- 856 Farrokhzadeh, S., Monfared, S.A.H., Azizian, G., Shahraki, A.S., Ertsen, M.W., Abraham, E., 2020.
857 Sustainable Water Resources Management in an Arid Area Using a Coupled Optimization-
858 Simulation Modeling. *Water* 2020, Vol. 12, Page 885 12, 885. <https://doi.org/10.3390/W12030885>
- 859 Ghaheri, M., Baghal-Vayjooee, M.H., Naziri, J., 1999. Lake Urmia, Iran: A summary review. *Int. J. Salt*
860 *Lake Res.* 8, 19–22. <https://doi.org/10.1023/A:1009062005606>
- 861 Hakami-Kermani, A., Babazadeh, H., Porhemmat, J., Sarai-Tabrizi, M., 2020. An uncertainty assessment
862 of reservoir system performance indices under the climate change effect. *Ain Shams Eng. J.*
863 <https://doi.org/10.1016/j.asej.2020.03.015>

- 864 Harbaugh, A.W., 2005. MODFLOW-2005, the US Geological Survey modular ground-water model: the
865 ground-water flow process. US Department of the Interior, US Geological Survey.
- 866 Hosseini-Moghari, S.-M., Araghinejad, S., Tourian, M.J., Ebrahimi, K., Döll, P., 2018. Quantifying the
867 impacts of human water use and climate variations on recent drying of Lake Urmia basin: the value
868 of different sets of spaceborne and in-situ data for calibrating a hydrological model. *Hydrol. Earth
869 Syst. Sci. Discuss.* 1–29. <https://doi.org/10.5194/hess-2018-318>
- 870 Hu, Z., Chen, Y., Yao, L., Wei, C., Li, C., 2016. Optimal allocation of regional water resources: From a
871 perspective of equity-efficiency tradeoff. *Resour. Conserv. Recycl.* 109, 102–113.
872 <https://doi.org/10.1016/j.resconrec.2016.02.001>
- 873 Jägermeyr, J., Pastor, A., Biemans, H., Gerten, D., 2017. Reconciling irrigated food production with
874 environmental flows for Sustainable Development Goals implementation. *Nat. Commun.* 8.
875 <https://doi.org/10.1038/ncomms15900>
- 876 Karamouz, M., Kerachian, R., Zahraie, B., 2004. Monthly water resources and irrigation planning: case
877 study of conjunctive use of surface and groundwater resources. *J. Irrig. ...* 391–402.
878 [https://doi.org/10.1061/\(ASCE\)0733-9437\(2004\)130:5\(391\)](https://doi.org/10.1061/(ASCE)0733-9437(2004)130:5(391))
- 879 Lemoalle, J., Bader, J.C., Leblanc, M., Sedick, A., 2012. Recent changes in Lake Chad: Observations,
880 simulations and management options (1973-2011). *Glob. Planet. Change* 80–81, 247–254.
881 <https://doi.org/10.1016/j.gloplacha.2011.07.004>
- 882 Loucks, D.P., van Beek, E., 2005. Appendix A : Natural System Processes and Interactions, *Water
883 Resources*.
- 884 Mainuddin, M., Kirby, M., Qureshi, M.E., 2007. Integrated hydrologic-economic modelling for analyzing
885 water acquisition strategies in the Murray River Basin. *Agric. Water Manag.* 93, 123–135.
886 <https://doi.org/10.1016/j.agwat.2007.06.011>
- 887 Malano, H.M., Davidson, B., 2009. A framework for assessing the trade-offs between economic and
888 environmental uses of water in a river basin. *Irrig. Drain.* 58, S133–S147.
889 <https://doi.org/10.1002/ird.484>
- 890 Mancosu, N., Snyder, R.L., Kyriakakis, G., Spano, D., 2015. Water scarcity and future challenges for
891 food production. *Water (Switzerland)* 7, 975–992. <https://doi.org/10.3390/w7030975>
- 892 Ministry of Energy of Iran, 2016. Implementation strategies for 40% reduction of Agricultural Water
893 Consumption in Zarrineh Rood and Simineh rood River basins, Vol. 7: Planning and management
894 studies of water resources and consumption in Miyandoab plain (available in Persian).
- 895 Molden, D., 2013. Water for food water for life: A Comprehensive assessment of water management in
896 agriculture, *Water for Food Water for Life: A Comprehensive Assessment of Water Management in
897 Agriculture*. <https://doi.org/10.4324/9781849773799>
- 898 Moshir Panahi, D., Kalantari, Z., Ghajarnia, N., Seifollahi-Aghmiuni, S., Destouni, G., 2020. Variability
899 and change in the hydro-climate and water resources of Iran over a recent 30-year period. *Sci. Rep.*
900 10, 1–9. <https://doi.org/10.1038/s41598-020-64089-y>
- 901 Munoz-Hernandez, A., Mayer, A.S., Watkins, D.W., 2011. Integrated Hydrologic-Economic-Institutional
902 Model of Environmental Flow Strategies for Rio Yaqui Basin, Sonora, Mexico. *J. Water Resour.
903 Plan. Manag.* 137, 227–237. [https://doi.org/10.1061/\(ASCE\)WR.1943-5452.0000108](https://doi.org/10.1061/(ASCE)WR.1943-5452.0000108)
- 904 Nalbantis, I., Tsakiris, · G, 2009. Assessment of Hydrological Drought Revisited. *Water Resour Manag.*
905 23, 881–897. <https://doi.org/10.1007/s11269-008-9305-1>

- 906 O’Keeffe, J., 2009. Sustaining river ecosystems: Balancing use and protection. *Prog. Phys. Geogr.* 33,
907 339–357. <https://doi.org/10.1177/0309133309342645>
- 908 Pang, A., Sun, T., Yang, Z., 2014. Cadre de détermination des débits environnementaux recommandé
909 conciliant les demandes en eau agricoles et les écosystèmes. *Hydrol. Sci. J.* 59, 890–903.
910 <https://doi.org/10.1080/02626667.2013.816425>
- 911 Pang, A., Sun, T., Yang, Z., 2013. Economic compensation standard for irrigation processes to safeguard
912 environmental flows in the Yellow River Estuary, China. *J. Hydrol.* 482, 129–138.
913 <https://doi.org/10.1016/j.jhydrol.2012.12.050>
- 914 Peralta, R.C., Cantiller, R.R.A., Terry, J.E., 1995. Optimal Large-Scale Conjunctive Water-Use Planning:
915 Case Study. *J. Water Resour. Plan. Manag.* 121, 471–478. [https://doi.org/10.1061/\(ASCE\)0733-9496\(1995\)121:6\(471\)](https://doi.org/10.1061/(ASCE)0733-9496(1995)121:6(471))
- 917 Pritchard, H.D., 2017. Asia’s glaciers are a regionally important buffer against drought. *Nature* 545.
918 2017, 169-174, <https://doi.org/10.1038/nature22062>
- 919 Pulido-Velazquez, M., Andreu, J., Sahuquillo, A., Pulido-Velazquez, D., 2008. Hydro-economic river
920 basin modelling: The application of a holistic surface-groundwater model to assess opportunity costs
921 of water use in Spain. *Ecol. Econ.* 66, 51–65. <https://doi.org/10.1016/j.ecolecon.2007.12.016>
- 922 Purkey, D., Galbraith, H., Huber-Lee, A., Sieber, J., Yates, D., 2009. WEAP21—A Demand-, Priority-,
923 and Preference-Driven Water Planning Model. *Water Int.* 30, 501–512.
924 <https://doi.org/10.1080/02508060508691894>
- 925 Raes, D., Geerts, S., Kipkorir, E., Wellens, J., Sahli, A., 2005. Simulation of yield decline as a result of
926 water stress with a robust soil water balance model. <https://doi.org/10.1016/j.agwat.2005.04.006>
- 927 Rumbaur, C., Thevs, N., Disse, M., Ahlheim, M., Brieden, A., Cyffka, B., Duethmann, D., Feike, T.,
928 Frör, O., Gärtner, P., Halik, Hill, J., Hinnenthal, M., Keilholz, P., Kleinschmit, B., Krysanova, V.,
929 Kuba, M., Mader, S., Menz, C., Othmanli, H., Pelz, S., Schroeder, M., Siew, T.F., Stender, V., Stahr,
930 K., Thomas, F.M., Welp, M., Wortmann, M., Zhao, X., Chen, X., Jiang, T., Luo, J., Yimit, H., Yu,
931 R., Zhang, X., Zhao, C., 2015. Sustainable management of river oases along the Tarim River
932 (SuMaRiO) in Northwest China under conditions of climate change. *Earth Syst. Dyn.* 6, 83–107.
933 <https://doi.org/10.5194/esd-6-83-2015>
- 934 Safavi, H.R., Darzi, F., Mariño, M.A., 2010. Simulation-optimization modeling of conjunctive use of
935 surface water and groundwater. *Water Resour. Manag.* 24, 1965–1988.
936 <https://doi.org/10.1007/s11269-009-9533-z>
- 937 Schoups, G., Addams, C.L., Gorelick, S.M., 2005. Multi-objective calibration of a surface water-
938 groundwater flow model in an irrigated agricultural region: Yaqui Valley, Sonora, Mexico. *Hydrol.*
939 *Earth Syst. Sci.* 9, 549–568. <https://doi.org/10.5194/hess-9-549-2005>
- 940 Schoups, G., Addams, C.L., Minjares, J.L., Gorelick, S.M., 2006. Sustainable conjunctive water
941 management in irrigated agriculture: Model formulation and application to the Yaqui Valley,
942 Mexico. *Water Resour. Res.* 42. <https://doi.org/10.1029/2006WR004922>
- 943 Schroeder, P.R., Dozier, T.S., Zappi, P.A., Mcenroe, B.M., Sjostrom, J.W., Peyton, R.L., 1994. The
944 hydrologic evaluation of landfill performance (Help) model.
- 945 Schulz, S., Darehshouri, S., Hassanzadeh, E., Tajrishy, M., Schüth, C., 2020. Climate change or irrigated
946 agriculture – what drives the water level decline of Lake Urmia. *Sci. Rep.* 10, 1–10.
947 <https://doi.org/10.1038/s41598-019-57150-y>

- 948 Seo, S.B., Mahinthakumar, G., Sankarasubramanian, A., Kumar, M., 2018. Conjunctive Management of
 949 Surface Water and Groundwater Resources under Drought Conditions Using a Fully Coupled
 950 Hydrological Model. *J. Water Resour. Plan. Manag.* 144, 04018060.
 951 [https://doi.org/10.1061/\(ASCE\)WR.1943-5452.0000978](https://doi.org/10.1061/(ASCE)WR.1943-5452.0000978)
- 952 Shadkam, S., Ludwig, F., van Vliet, M.T.H., Pastor, A., Kabat, P., 2016. Preserving the world second
 953 largest hypersaline lake under future irrigation and climate change. *Sci. Total Environ.* 559, 317–
 954 325. <https://doi.org/10.1016/j.scitotenv.2016.03.190>
- 955 Sieber, J., Purkey, D., 2015. WEAP Water Evaluation and Planning System: User Guide, Stockholm
 956 Environment Institute, US Center.
- 957 Singh, A., 2014. Simulation-optimization modeling for conjunctive water use management. *Agric. Water*
 958 *Manag.* 141, 23–29. <https://doi.org/10.1016/j.agwat.2014.04.003>
- 959 Singh, A., Panda, S.N., 2013. Optimization and Simulation Modelling for Managing the Problems of
 960 Water Resources. *Water Resour. Manag.* 27, 3421–3431. <https://doi.org/10.1007/s11269-013-0355-7>
- 961 Sisto, N.P., 2009. Environmental flows for rivers and economic compensation for irrigators. *J. Environ.*
 962 *Manage.* 90, 1236–1240. <https://doi.org/10.1016/j.jenvman.2008.06.005>
- 963 Smakhtin, V.U., Shilpakar, R.L., Hughes, D.A., 2006. Hydrology-based assessment of environmental
 964 flows: An example from Nepal. *Hydrol. Sci. J.* 51, 207–222. <https://doi.org/10.1623/hysj.51.2.207>
- 965 Srinivasa Prasad, A., Umamahesh, N. V., Viswanath, G.K., 2006. Optimal irrigation planning under water
 966 scarcity. *J. Irrig. Drain. Eng.* 132, 228–237. [https://doi.org/10.1061/\(ASCE\)0733-
 967 9437\(2006\)132:3\(228\)](https://doi.org/10.1061/(ASCE)0733-9437(2006)132:3(228))
- 968 Tennant, D.L., 1976. Instream Flow Regimens for Fish, Wildlife, Recreation and Related Environmental
 969 Resources. *Fisheries* 1, 6–10. [https://doi.org/10.1577/1548-8446\(1976\)001<0006:ifrffw>2.0.co;2](https://doi.org/10.1577/1548-8446(1976)001<0006:ifrffw>2.0.co;2)
- 970 Tharme, R.E., 2003. A global perspective on environmental flow assessment: Emerging trends in the
 971 development and application of environmental flow methodologies for rivers. *River Res. Appl.* 19,
 972 397–441. <https://doi.org/10.1002/rra.736>
- 973 Tian, Y., Zheng, Y., Zheng, C., Xiao, H., Fan, W., Zou, S., Wu, B., Yao, Y., Zhang, A., Liu, J., 2015.
 974 Exploring scale-dependent ecohydrological responses in a large endorheic river basin through
 975 integrated surface water-groundwater modeling. *Water Resour. Res.* 51, 4065–4085.
 976 <https://doi.org/10.1002/2015WR016881>
- 977 Valipour, M., 2015. A comprehensive study on irrigation management in Asia and Oceania. *Arch. Agron.*
 978 *Soil Sci.* 61, 1247–1271. <https://doi.org/10.1080/03650340.2014.986471>
- 979 Valipour, M., Ziatabar Ahmadi, M., Raeini-Sarjaz, M., Gholami Sefidkouhi, M.A., Shahnazari, A.,
 980 Fazlola, R., Darzi-Naftchali, A., 2015. Agricultural water management in the world during past half
 981 century. *Arch. Agron. Soil Sci.* 61, 657–678. <https://doi.org/10.1080/03650340.2014.944903>
- 982 Wang, J., Song, C., Reager, J.T., Yao, F., Famiglietti, J.S., Sheng, Y., MacDonald, G.M., Brun, F.,
 983 Schmied, H.M., Marston, R.A., Wada, Y., 2018. Recent global decline in endorheic basin water
 984 storages. *Nat. Geosci.* 11, 926–932. <https://doi.org/10.1038/s41561-018-0265-7>
- 985 Wei, Y., Davidson, B., Chen, D., White, R., 2009. Balancing the economic, social and environmental
 986 dimensions of agro-ecosystems: An integrated modeling approach. *Agric. Ecosyst. Environ.* 131,
 987 263–273. <https://doi.org/10.1016/j.agee.2009.01.021>
- 988 Xevi, E., Khan, S., 2005. A multi-objective optimisation approach to water management. *J. Environ.*
 989 *Manage.* 77, 269–277. <https://doi.org/10.1016/j.jenvman.2005.06.013>

- 990 Xue, J., Gui, D., Lei, J., Sun, H., Zeng, F., Feng, X., 2017. A hybrid Bayesian network approach for
991 trade-offs between environmental flows and agricultural water using dynamic discretization. *Adv.*
992 *Water Resour.* 110, 445–458. <https://doi.org/10.1016/j.advwatres.2016.10.022>
- 993 Yang, W., Yang, Z., 2014. Analyzing hydrological regime variability and optimizing environmental flow
994 allocation to lake ecosystems in a sustainable water management framework: Model development
995 and a case study for china’s baiyangdian watershed. *J. Hydrol. Eng.* 19, 993–1005.
996 [https://doi.org/10.1061/\(ASCE\)HE.1943-5584.0000874](https://doi.org/10.1061/(ASCE)HE.1943-5584.0000874)
- 997 Yapiyev, V., Sagintayev, Z., Inglezakis, V.J., Samarkhanov, K., Verhoef, A., 2017. Essentials of
998 endorheic basins and lakes: A review in the context of current and futurewater resource management
999 and mitigation activities in Central Asia. *Water (Switzerland)* 9, 798.
1000 <https://doi.org/10.3390/w9100798>
- 1001 Yasi, M., Ashori, M., 2017. Environmental Flow Contributions from In-Basin Rivers and Dams for
1002 Saving Urmia Lake. *Iran. J. Sci. Technol. Trans. Civ. Eng.* 41, 55–64.
1003 <https://doi.org/10.1007/s40996-016-0040-1>
- 1004

Supplementary material to

Meeting agricultural and environmental water demand in endorheic irrigated river basins: a simulation-optimization approach applied to the Urmia Lake basin in Iran

Amir Hossein Dehghanipour^{a,*}, Gerrit Schoups^b, Bagher Zahabiyoun^{a,*}, Hossein Babazadeh^c

^a *Department of Water Management, School of Civil Engineering, Iran University of Science and Technology, Tehran, Iran*

^b *Department of Water Management, Faculty of Civil Engineering and Geosciences, Delft University of Technology, Delft, The Netherlands*

^c *Department of Water Science and Engineering, Science and Research Branch, Islamic Azad University, Tehran, Iran*

* Corresponding author address: Department of Water Management, School of Civil Engineering, Iran University of Science and Technology, Narmak, Tehran, Iran, Postal Code: 16846-13114.

E-mail: A.Dehghanipour@tudelft.nl (A.H. Dehghanipour), Bagher@iust.ac.ir (B. Zahabiyoun)

¹Present address: Department of Water Management, Faculty of Civil Engineering and Geosciences, Delft University of Technology, Stevinweg 1, 2628CN, Delft, Netherlands.

32 **1.Introduction**

33 The supplementary material includes additional Figures (Fig. S1 to S7), Tables (Table S1 to S6), and text
 34 to enhance our article. Table S1 presents a summary of previous studies that applied simulation-
 35 optimization to find water allocation strategies that simultaneously meet environmental flow requirements
 36 and water demand from agriculture and other users. Table S2, Table S3, and Fig. S1 present crop
 37 characteristics for the Miyandoab Plain and Fig. S2 shows the annual observed river discharge upstream
 38 of Bukan reservoir. Finally, Fig. S3 to S7 and Table S4 to S6 provide additional information on results
 39 and discussion in the paper.

40 **Table S1: Some studies applied the optimization model to evaluate environmental flow requirements**

Study	Objective Function	Case study	Environmental flow requirement	
			Implementation in the optimization	Calculation method
Xevi and Khan (2005)	<ul style="list-style-type: none"> • maximize agricultural net profit • minimize variable cost • minimize total groundwater withdrawal to meet agricultural demand 	hypothetical Irrigation Area using real data of Berembed Weir on the Murrumbidgee River in Australia	As a firm constraint	Downstream measured river discharge
Pulido-Velazquez et al. (2008)	<ul style="list-style-type: none"> • minimize the total cost of water distribution and system operation in the agricultural and urban sectors 	Adra River Basin in Spain	as a firm constraint	Unknown
Anghileri et al. (2013)	<ul style="list-style-type: none"> • minimize deficit irrigation • maximize hydropower generation 	Alpine watershed in Italy	as a firm constraint	function of the reservoir storage
Yang and Yang (2014)	<ul style="list-style-type: none"> • maximize the net benefit for the industrial sectors • minimize the absolute deviation of the calculated lake water level from the natural level • minimize the crop yield losses 	Lake Baiyangdian basin in China	as an objective function	was not considered
Roozbahani et al. (2015)	<ul style="list-style-type: none"> • maximize the profit of agricultural, urban, and industrial sectors • minimize the shortage of supply environmental flow requirements • maximizes allocated water to the social aspect 	Sefidrud Basin in Iran	as an objective function	Using Tennant method
Hu et al. (2016)	<ul style="list-style-type: none"> • maximize the economic benefit efficiency from water allocation • maximize water allocation equity by using the Gini coefficient 	Qujiang river basin in China	as a firm constraint	Using Tennant method
Fallah-Mehdipour et al. (2018)	<ul style="list-style-type: none"> • minimized deviation between the installed capacity of the power plant and generated power • minimized the absolute difference between the environmental flow requirement and reservoir release 	Karoon Basin in Iran	as an objective function	Using Tennant method
Fallah-Mehdipour et al. (2020)	<ul style="list-style-type: none"> • maximize supply water for agricultural demand • maximize supply water for environmental flow requirements • maximize supply water for urban demand 	Karkhe Basin in southwestern Iran	as an objective function	Using Tennant method
Our study	<ul style="list-style-type: none"> • maximize agricultural net profit • maximize agricultural sustainability • maximize inflow to the Lake 	Urmia lake basin in Iran	as an objective function	Decision variable in the optimization model

41
 42
 43
 44
 45
 46
 47
 48
 49
 50
 51
 52

53 2. Case study

54
55
56Table S2: Growing Stage Length, Crop coefficients (k_c), and Maximum root depth for crops in Miyandoab Plain according to FAO Irrigation and Drainage (Allen et al., 1998)

Crop or Orchards	Stage Length (day)				k_c			Root Depth (m)	ETp (m ³ /hec)
	Initial	Development	Midseason	Late	Initial	Midseason	Late		
Alfalfa (1st cutting cycle)	10	30	25	10	0.4	0.95	0.9	1.5	8730.36
Alfalfa (2st, 3st, 4st cutting cycle)	5	20	10	10	0.4	0.95	0.9	1.5	
Wheat	30	140	40	30	0.4	1.15	0.3	1.65	5199.79
Maize	25	40	45	30	0.15	1.2	0.5	1.35	6373.55
Tomato	25	40	60	30	0.15	1.15	0.8	1.1	6701.28
Sugar beet	35	60	70	40	0.35	1.2	0.7	0.95	9048.52
Canola	20	120	30	30	0.35	1.2	0.35	1.25	3248.65
Sorghum	25	35	40	30	0.4	1.1	0.75	1.5	5336.50
Saffron	30	45	70	55	0.4	0.85	0.55	0.45	2922.84

57
58
59
60
61
62
63
64
65Table S3: Maximum yield (Y_m), market price, and cost of crops in Miyandoab Plain (Ministry of Energy of Iran, 2016).
Yields and prices are listed for first (e.g. grain) and second (e.g. straw) harvests.

Crop	First harvest		Second harvest		Cost (USD/ha)	Maximum net profit (USD/ha)
	Yield Y_{m1} (Kg/ha)	Market price 1 (USD/Kg)	Yield Y_{m2} (Kg/ha)	Market price 2 (USD/Kg)		
Wheat	5500	0.46	6600	0.08	797.96	2260
Maize	10300	0.38	5950	0.06	1288.92	3023
Alfalfa	13000	0.32	0	0	1365.2	2795
Tomato	50000	0.14	0	0	3229.2	3771
Sugar beet	70000	0.11	0	0	3001.76	4558
Canola	3100	0.88	2402	0.08	950.8	1969
Sorghum	97000	0.06	0	0	1322.92	4109
Saffron	10	2000	18948	0.04	3637.96	13120

67
68

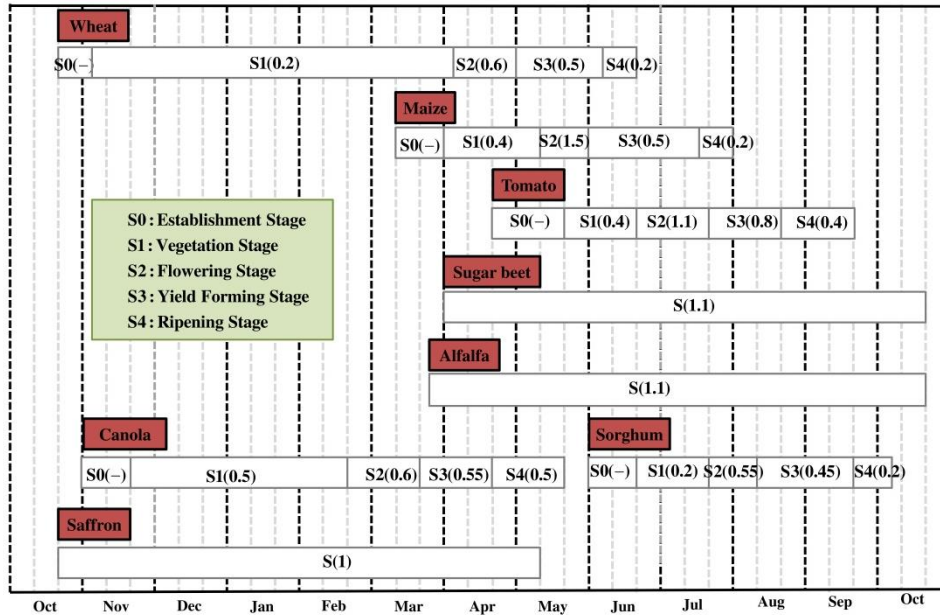


Fig. S1: Calendar and growth stages (S0-S4) for crops in the Miyandoab Plain. Values in brackets are the crop yield response factors ($k_{y,i}$ in Eq. 2) for each crop stage (Ministry of Energy of Iran, 2016; Steduto et al., 2012).

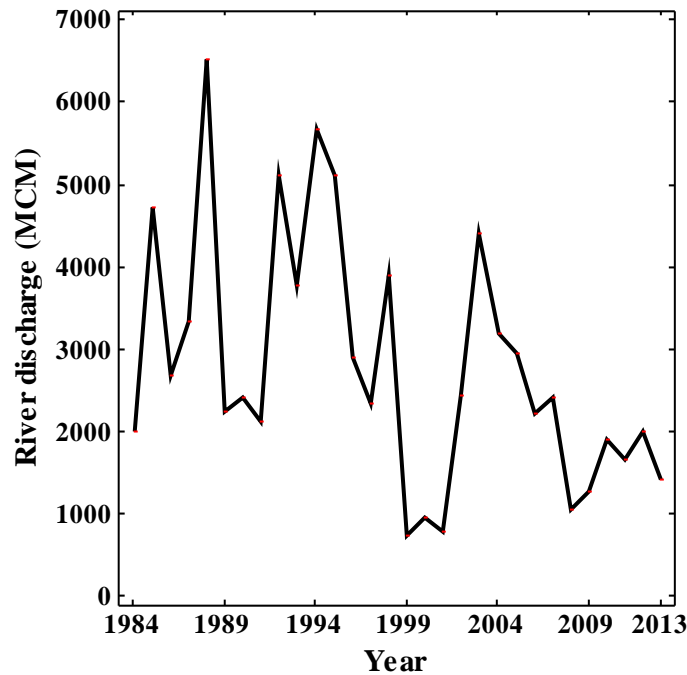


Fig. S2: Time series of annual observed river discharge upstream of Bukan reservoir

3. Results and discussion

The integrated simulation-optimization model includes 5000 simulation runs for each strategy. In this study, we used WEAP (version 2019), MODFLOW 2005, and MATLAB (version 2018) to develop the simulation-optimization model. Each simulation run for the period (1984-2013) takes on average 7 min on a standard desktop system with CPU speed of 3.7 GHz and 16 GB of memory installed (RAM).

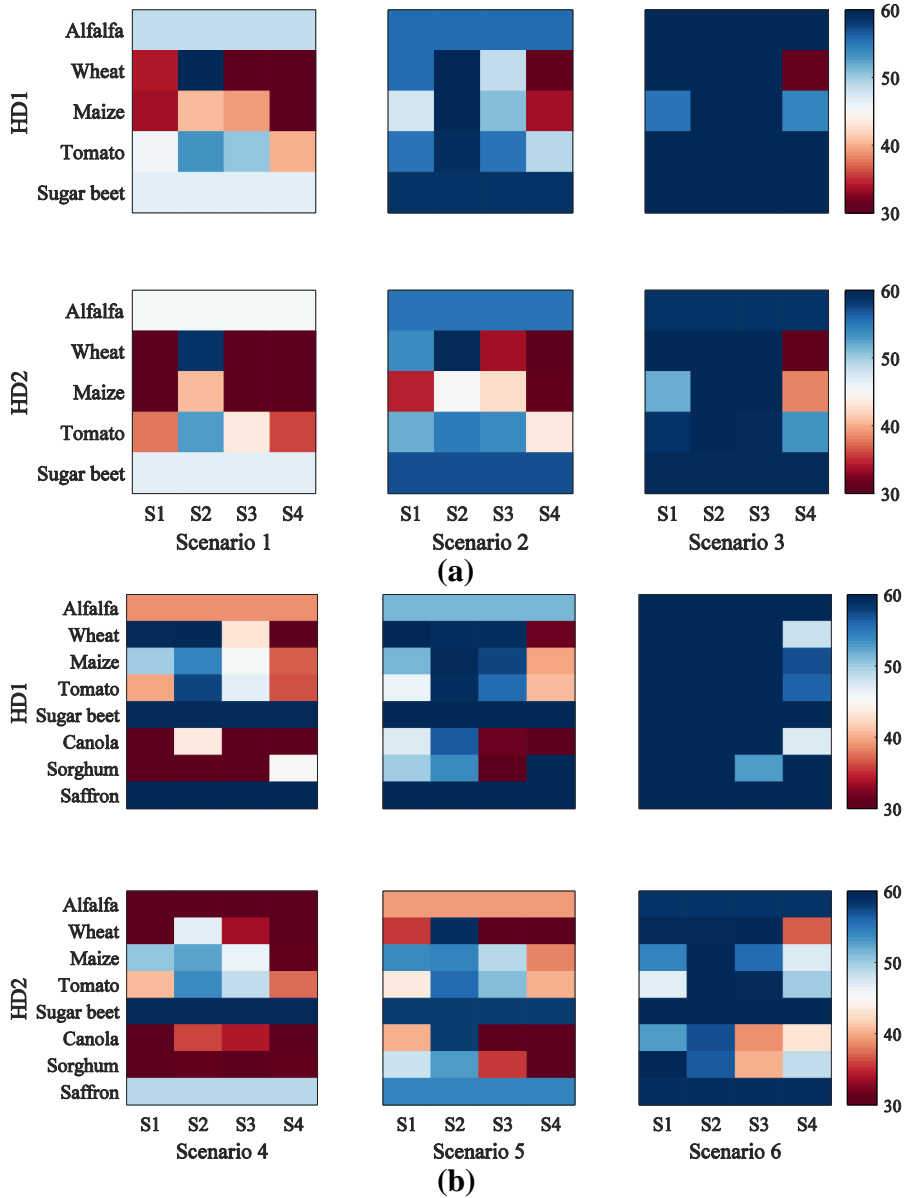
Fig. S3.a and S3.b show heat maps of the intervention point (Z_{int}), i.e. relative soil water content that triggers irrigation, for each growth stage of each crop in current and proposed crop patterns in strategy I,

84 respectively (for HD1 and HD2 years; crop acreages for HD3 years were near zero). As mentioned
85 before, irrigation starts when relative soil water content falls below the intervention point. Therefore,
86 decreasing the intervention point results in more deficit irrigation, less water withdrawal for irrigation,
87 and more crop water stress. Value of the intervention point increases from scenarios 1 to 3 (scenarios 4 to
88 6). Therefore, water withdrawal for irrigation increases from scenarios 1 to 3 (scenarios 4 to 6) (Table S4
89 and Table S5), resulting in an increase of the Economic agricultural index and a decrease of the
90 Environmental index (Fig. 7.a). Furthermore, the intervention point decreases from HD1 to HD2, i.e. drier
91 conditions lead to more deficit irrigation.

92 The application of deficit irrigation varies by crop. Drought-resistant crops like wheat, with values for
93 yield response factor K_y less than 1 in each growth stage (Fig. S1), are more suited for deficit irrigation,
94 than drought-sensitive crops like sugar beet and saffron, with yield response factor values greater than 1.
95 These crop differences are reflected in the optimal values of z_{int} in Fig. S3, which are high for sugar beet
96 and saffron, and low for wheat.

97 Furthermore, the application of deficit irrigation is sensitive to the growth stage. For instance, the
98 intervention point of stage 2 (vegetation stage) of maize and tomato is higher than other stages, because
99 of the yield response factor (K_y) of this stage is higher than 1, and this stage is sensitive to deficit
100 irrigation. On the other hand, the intervention points of stage 4 (ripening stage) of wheat, maize, and
101 tomato are lower compared to other stages. The yield response factor (K_y) of this stage is smallest, and
102 thus deficit irrigation is applied in stage 4.

103
104
105
106
107
108
109



110 Fig. S3: Values for the intervention point z_{int} for each growth stage of each crop of six selected scenarios on the Pareto
 111 front of strategy I: (a) current crop pattern, and (b) proposed crop pattern. HD1, HD2, HD3 are hydrological
 112 conditions: non-drought, mild drought, and moderate drought, respectively. Historically, the value of z_{int} is 45%.
 113

114 Table S4: Time-averaged (1984-2013) root-zone water balance components (in MCM) for agricultural zones within the
 115 Miyandoab aquifer boundary for the six Pareto scenarios of strategy I.

Parameter		Historical	scenario 1	scenario 2	scenario 3	scenario 4	scenario 5	scenario 6
Inflow	Effective precipitation	218.68	218.68	218.68	218.68	218.68	218.68	218.68
	SW extraction for irrigation	763.79	721.04	807.4	907.74	598.06	722.28	848.65
	GW extraction for irrigation	136.82	126.48	133.21	133.93	110.23	116.16	123.01
	Total inflows	1119.28	1066.2	1159.29	1260.35	926.97	1057.12	1190.34
Outflow	ET actual	366.26	347.39	368.15	373.81	315.03	330.67	349.64
	Surface runoff+Interflow	561.14	552.19	605.06	678.55	459.59	549.14	633.17
	GW recharge	182.67	166	180.53	191.25	148.43	166.45	186.25
	Total outflows	1110.06	1065.58	1153.75	1243.61	923.05	1046.27	1169.06
Storage change		9.22	0.62	5.54	16.74	3.92	10.85	21.27

116
 117
 118

119
120

Table S5: Simulated time-averaged (1984-2013) root-zone water balance components (in MCM) for agricultural zones outside of the Miyandoab aquifer boundary for six selected scenarios in the Pareto front in strategy I.

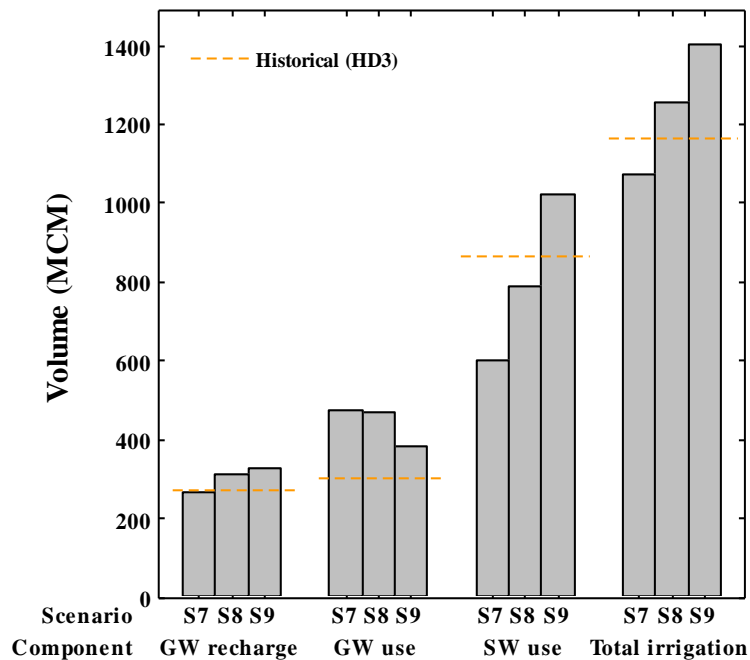
Parameter		Historical	Scenario 1	Scenario 2	Scenario 3	Scenario 4	Scenario 5	Scenario 6
Inflow	Effective precipitation	116.97	116.97	116.97	116.97	116.97	116.97	116.97
	SW extraction for irrigation	174.74	168.39	181.66	199.73	156.56	177.48	202.24
	GW extraction for irrigation	197.21	186.39	192.09	191.06	172.86	180.59	187.52
	Total inflows	488.92	471.75	490.72	507.76	446.4	475.05	506.73
Outflow	ET actual	185.09	180.69	183.82	185.96	172.52	176.7	181.55
	Surface runoff + Interflow	194.84	190.3	199.14	211.27	173.96	191.79	209.85
	GW recharge	107.5	102.21	106.47	108.98	99.95	105.12	110.51
	Total outflows	487.43	473.2	489.42	506.22	446.43	473.6	501.9
Storage change		1.49	-1.44	1.3	1.54	-0.03	1.44	4.82

121
122
123

Table S6: The value of GW capacity and crop acreage in HD3 in scenarios 7 to 9.

Variable		scenario 7	scenario 8	scenario 9
Area	HD1	similar scenario 4-HD1	similar scenario 5-HD1	similar scenario 6-HD1
	HD2	similar scenario 4-HD2	similar scenario 5-HD2	similar scenario 6-HD2
	HD3	Current Area	Current Area	Current Area
Zint	HD1	similar scenario 4-HD1	similar scenario 5-HD1	similar scenario 6-HD1
	HD2	similar scenario 4-HD2	similar scenario 5-HD2	similar scenario 6-HD2
	HD3	similar scenario 4-HD2	similar scenario 5-HD2	similar scenario 6-HD2
MFR		similar scenario 4	similar scenario 5	similar scenario 6
GW capacity	HD1	No change	No change	No change
	HD2	No change	No change	No change
	HD3	Increase until 2 time	Increase until 2 time	Increase until 2 time

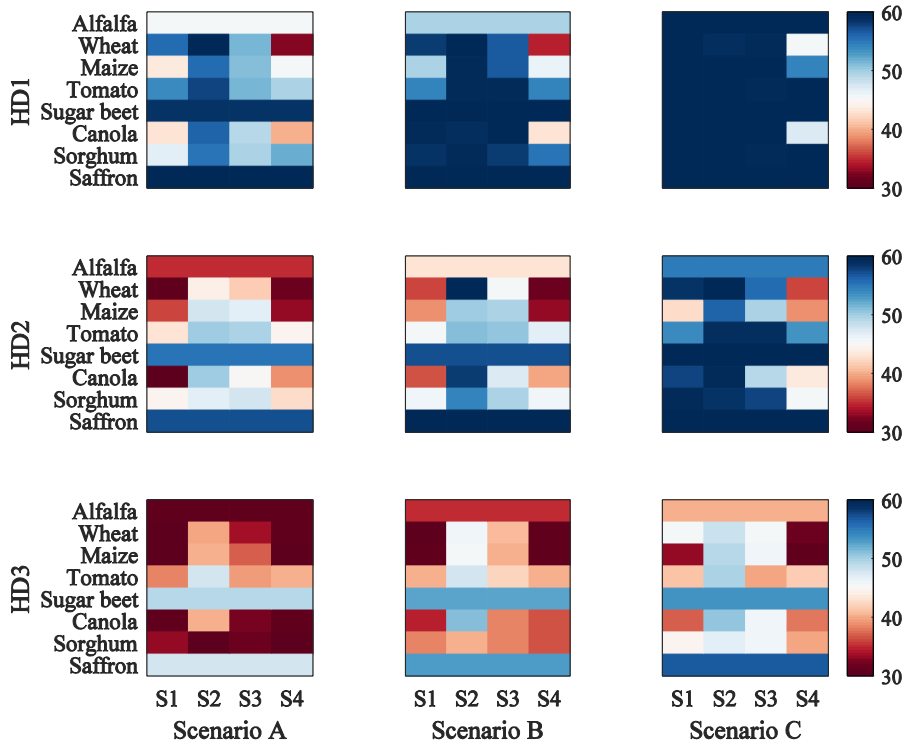
124
125



126
127

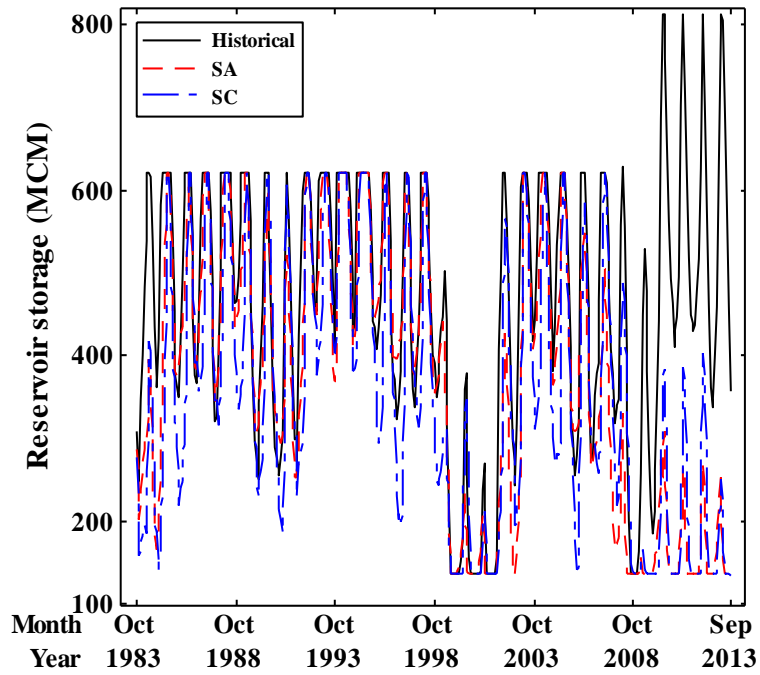
Fig. S4: Water balance components for scenarios 7-9 in HD3 years (moderate drought)

128
129



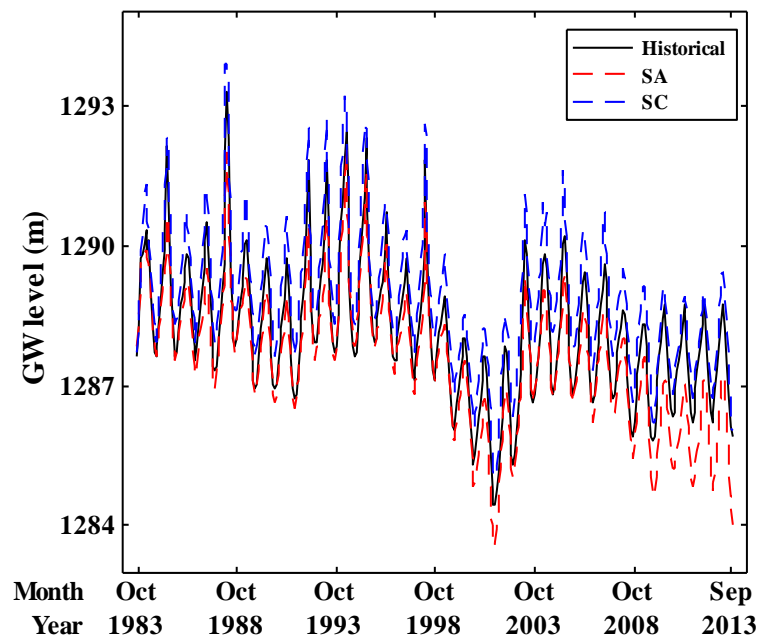
130
131
132
133
134
135

Fig. S5: Values for intervention point z_{int} for each growth stage of each crop of three selected scenarios on the Pareto front of strategy II



136
137
138
139
140

Fig. S6: Monthly Bukan reservoir storage for three selected scenarios on the Pareto front of strategy II.



141
142
143 **Fig. S7: Monthly GW levels for three selected scenarios on the Pareto front of strategy II.**

144
145 **References**

- 146 Allen, R.G., Pereira, L.S., Raes, D., Smith, M., 1998. FAO Irrigation and drainage paper No. 56. Rome: Food and Agriculture
147 Organization of the United Nations.
- 148 Anghileri, D., Castelletti, A., Pianosi, F., Soncini-Sessa, R., Weber, E., 2013. Optimizing watershed management by
149 coordinated operation of storing facilities. *J. Water Resour. Plan. Manag.* 139, 492–500.
150 [https://doi.org/10.1061/\(ASCE\)WR.1943-5452.0000313](https://doi.org/10.1061/(ASCE)WR.1943-5452.0000313)
- 151 Fallah-Mehdipour, E., Bozorg-Haddad, O., Loáiciga, H.A., 2020. Climate-environment-water: integrated and non-integrated
152 approaches to reservoir operation. *Environ. Monit. Assess.* 192. <https://doi.org/10.1007/s10661-019-8039-2>
- 153 Fallah-Mehdipour, E., Bozorg-Haddad, O., Loáiciga, H.A., 2018. Calculation of multi-objective optimal tradeoffs between
154 environmental flows and hydropower generation. *Environ. Earth Sci.* 77. <https://doi.org/10.1007/s12665-018-7645-6>
- 155 Hu, Z., Chen, Y., Yao, L., Wei, C., Li, C., 2016. Optimal allocation of regional water resources: From a perspective of equity-
156 efficiency tradeoff. *Resour. Conserv. Recycl.* 109, 102–113. <https://doi.org/10.1016/j.resconrec.2016.02.001>
- 157 Ministry of Energy of Iran, 2016. Implementation strategies for 40% reduction of Agricultural Water Consumption in Zarrineh
158 Roud and Simineh road River basins, Vol. 7: Planning and management studies of water resources and consumption in
159 Miyandoab plain (available in Persian).
- 160 Pulido-Velazquez, M., Andreu, J., Sahuquillo, A., Pulido-Velazquez, D., 2008. Hydro-economic river basin modelling: The
161 application of a holistic surface-groundwater model to assess opportunity costs of water use in Spain. *Ecol. Econ.* 66,
162 51–65. <https://doi.org/10.1016/j.ecolecon.2007.12.016>
- 163 Roozbahani, R., Schreider, S., Abbasi, B., 2015. Optimal water allocation through a multi-objective compromise between
164 environmental, social, and economic preferences. *Environ. Model. Softw.* 64, 18–30.
165 <https://doi.org/10.1016/j.envsoft.2014.11.001>
- 166 Steduto, P., Hsiao, T.C., Fereres, E., Raes, D., 2012. Crop yield response to water, FAO Irrigation and Drainage Paper No.66.
- 167 Xevi, E., Khan, S., 2005. A multi-objective optimisation approach to water management. *J. Environ. Manage.* 77, 269–277.
168 <https://doi.org/10.1016/j.jenvman.2005.06.013>
- 169 Yang, W., Yang, Z., 2014. Analyzing hydrological regime variability and optimizing environmental flow allocation to lake
170 ecosystems in a sustainable water management framework: Model development and a case study for china's baiyangdian
171 watershed. *J. Hydrol. Eng.* 19, 993–1005. [https://doi.org/10.1061/\(ASCE\)HE.1943-5584.0000874](https://doi.org/10.1061/(ASCE)HE.1943-5584.0000874)